Tenascin C in the tumor-nerve microenvironment enhances perineural invasion and correlates with locoregional recurrence in pancreatic ductal adenocarcinoma

Pancreas

Tenascin C in the Tumor-Nerve Microenvironment Enhances Perineural invasion and Correlates With Locoregional Recurrence in Pancreatic Ductal Adenocarcinoma

--Manuscript Draft--

Manuscript Number:	PANCREAS 19189R1
Full Title:	Tenascin C in the Tumor-Nerve Microenvironment Enhances Perineural invasion and Correlates With Locoregional Recurrence in Pancreatic Ductal Adenocarcinoma
Short Title:	Tenascin C in Perineural Invasion of PDAC
Article Type:	Full Manuscript
Keywords:	pancreatic ductal adenocarcinoma; perineural invasion; tenascin C; dorsal root ganglion; tumor-nerve microenvironment; neurotropism
Corresponding Author:	Takanori Sakaguchi, M.D. Hamamatsu University School of Medicine Hamamatsu, JAPAN
Corresponding Author Secondary Information:	
Corresponding Author's Institution:	Hamamatsu University School of Medicine
Corresponding Author's Secondary Institution:	
First Author:	Satoru Furuhashi, MD
First Author Secondary Information:	
Order of Authors:	Satoru Furuhashi, MD
	Takanori Sakaguchi, MD, PhD
	Tomohiro Murakami, MD, PhD
	Mayu Fukushima, MD
	Yoshifumi Morita, MD, PhD
	Koji Ikegami, PhD
	Hirotoshi Kikuchi, MD, PhD
	Mitsutoshi Setou, MD, PhD
	Hiroya Takeuchi, MD, PhD
Order of Authors Secondary Information:	
Manuscript Region of Origin:	JAPAN
Abstract:	Objectives: Perineural invasion (PNI) is common in pancreatic ductal adenocarcinoma (PDAC) and worsens the postoperative prognosis. Tenascin C (TNC), an extracellular matrix glycoprotein, modulates tumor progression. We evaluated the functional roles of TNC, especially in PNI of PDAC. Methods: We examined immunohistochemical TNC expression in 78 resected PDAC specimens. The relationships between TNC expression and clinicopathological features were retrospectively analyzed. Interactions between cancer cells and TNC-supplemented nerves were investigated using an in vitro co-culture model with PDAC cell line and mouse dorsal root ganglion (DRG). Results: Tenascin C expression was predominant in perineural sites at invasive tumor front. High perineural TNC expression in 30 patients (38%) was associated with PNI, pathological T stage ≥ 3, and postoperative locoregional recurrence. High TNC expression was independently associated with postoperative, poor recurrence-free survival by multivariate analysis. In the in vitro co-culture model, a TNC-rich matrix enhanced both PDAC cell colony extensions toward nerves and DRG axonal outgrowth toward cancer cell colonies, whereas TNC did not affect axonal outgrowth or

	cancer cell proliferation in separately cultured DRG and PDAC cells. Conclusions: Strong perineural TNC expression indicated poor prognosis with locoregional recurrence. The neurotropism of TNC-induced PDAC suggests TNC is a potential PDAC therapeutic target.

Tenascin C in the Tumor-Nerve Microenvironment Enhances Perineural Invasion and Correlates With Locoregional Recurrence in Pancreatic Ductal Adenocarcinoma

Authors

Satoru Furuhashi MD

Second Department of Surgery and International Mass Imaging Center and Department of Cellular and Molecular Anatomy, Hamamatsu University School of Medicine, Hamamatsu, Shizuoka, Japan

Takanori Sakaguchi MD, PhD

Second Department of Surgery, Hamamatsu University School of Medicine, Hamamatsu, Shizuoka, Japan

Tomohiro Murakami MD, PhD

Second Department of Surgery, Hamamatsu University School of Medicine, Hamamatsu, Shizuoka, Japan

Mayu Fukushima MD

Department of Pathology, Hamamatsu University School of Medicine, Hamamatsu, Shizuoka, Japan

Yoshifumi Morita MD, PhD

Second Department of Surgery, Hamamatsu University School of Medicine,
Hamamatsu, Shizuoka, Japan

Koji Ikegami PhD

International Mass Imaging Center and Department of Cellular and Molecular Anatomy,
Hamamatsu University School of Medicine, Hamamatsu, Shizuoka, Japan

Hirotoshi Kikuchi MD, PhD

Second Department of Surgery, Hamamatsu University School of Medicine,
Hamamatsu, Shizuoka, Japan

Mitsutoshi Setou MD, PhD

International Mass Imaging Center and Department of Cellular and Molecular Anatomy;
Preeminent Medical Photonics Education and Research Center, Hamamatsu University
School of Medicine, Hamamatsu, Shizuoka, Japan; and Department of Anatomy, The
University of Hong Kong, China

Hiroya Takeuchi MD, PhD

Second Department of Surgery, Hamamatsu University School of Medicine,
Hamamatsu, Shizuoka, Japan

Corresponding author:

Takanori Sakaguchi, Second Department of Surgery, Hamamatsu University School of Medicine, 1-20-1 Handayama, Higashi-ku, Hamamatsu, Shizuoka, 431-3192, Japan

Telephone: +81-53-435-2279; Fax number: +81-53-435-2273; E-mail address: saka1119@hama-med.ac.jp

Running Title: Tenascin C in Perineural Invasion of PDAC

Funding: This study was supported by a Grant-in-Aid for Scientific Research (grant number 17K10694) from the Ministry of Education, Culture, Sports, Science and Technology of Japan. This work was also supported by MEXT/Japan Society for the Promotion of Science KAKENHI (grant number JP15H05898B1) and the Imaging Platform supported by the Ministry of Education, Culture, Sports, Science and Technology (MEXT), Japan and AMED (grant number JP18gm0910004).

Abstract:

Objectives: Perineural invasion (PNI) is common in pancreatic ductal adenocarcinoma (PDAC) and worsens the postoperative prognosis. Tenascin C (TNC), an extracellular matrix glycoprotein, modulates tumor progression. We evaluated the functional roles of TNC, especially in PNI of PDAC.

Methods: We examined immunohistochemical TNC expression in 78 resected PDAC specimens. The relationships between TNC expression and clinicopathological features were retrospectively analyzed. Interactions between cancer cells and TNC-supplemented nerves were investigated using an *in vitro* co-culture model with PDAC cell line and mouse dorsal root ganglion (DRG).

Results: Tenascin C expression was predominant in perineural sites at invasive tumor front. High perineural TNC expression in 30 patients (38%) was associated with PNI, pathological T stage ≥ 3, and postoperative locoregional recurrence. High TNC expression was independently associated with postoperative, poor recurrence-free survival by multivariate analysis. In the *in vitro* co-culture model, a TNC-rich matrix enhanced both PDAC cell colony extensions toward nerves and DRG axonal outgrowth toward cancer cell colonies, whereas TNC did not affect axonal outgrowth or cancer cell proliferation in

separately cultured DRG and PDAC cells.

Conclusions: Strong perineural TNC expression indicated poor prognosis with locoregional recurrence. The neurotropism of TNC-induced PDAC suggests TNC is a potential PDAC therapeutic target.

Keywords: pancreatic ductal adenocarcinoma, perineural invasion, tenascin C, dorsal root ganglion, tumor-nerve microenvironment, neurotropism

Introduction

Pancreatic ductal adenocarcinoma (PDAC) is one of the most aggressive malignancies, has a dismal prognosis, and is expected to become the second-highest cancer-related mortality by 2030 in the United States.[1] Most PDACs are unresectable at diagnosis because of locoregional spread or metastatic dissemination.[2] Even after curative resection by surgical intervention, recurrence frequently occurs and is strongly refractory to chemotherapeutic agents.[3] Thus, improved recognition of the pathology of PDAC, in particular, the aggressive nature of its invasion is warranted.

Perineural invasion (PNI) is a common pathological characteristic of PDAC and is seen in 70.8% to 93% of surgical PDAC specimens.[4,5] The presence of PNI in PDAC is associated with local recurrence [6-8] and can serve as an important prognostic factor.[9,10] Perineural invasion is also linked to cancer-related refractory pain that markedly impairs patients' quality of life.[11] During PNI progression, the nerve sheath has been proposed as the path of least resistance for tumor spreading.[12] More recently, based on neurotropic theory, the nerves and invading tumor cells can interact with each other through neurotrophins.[13] However, the detailed molecular mechanisms of PNI development in PDAC remain unclear.

Tenascin C (TNC) is an extracellular matrix glycoprotein that is tightly regulated in normal adult tissues,[14] is expressed during organogenesis (particularly in the developing central nervous system) and in migrating neural crest cells, and promotes tissue healing at injury sites. [15-17] In various malignant neoplasms, TNC is abundantly expressed in cancer stroma and its overexpression correlates with tumor progression and poor prognosis.[18-21] In pancreatic cancer, TNC is mainly synthesized by activated pancreatic stellate cells (PSCs) [22] and modulates tumor progression. [23] However, the relationship between TNC and PNI in PDAC has not been reported.

In this study, we hypothesized that TNC enhances PNI in PDAC. Therefore, we immunohistochemically examined TNC expression in resected PDAC specimen and clarified TNC abundance-related clinicopathologic factors. Moreover, we demonstrated a physiological role of TNC in PNI, using an *in vitro* co-culture model with a PDAC cell line and mouse dorsal root ganglion (DRG).

Material and Methods

Patients

Ninety-six patients with malignant pancreatic tumors who underwent surgery at our institute from April 2000 to June 2017 were enrolled in this study. We excluded patients with any preoperative treatment (n = 3), remnant pancreatic resection (n = 1), macroscopic residual tumor (R2 resection), distant metastasis (pathological M1 stage; n = 3), or other histological types including intraductal papillary mucinous carcinoma (n = 5), intraductal tubulopapillary carcinoma (n = 1), anaplastic adenocarcinoma (n = 1), and acinar cell adenocarcinoma (n = 1). Three patients were also excluded because of loss to follow up or death by other causes within 3 months postoperatively. Thus, 78 patients who were histologically diagnosed with PDAC were included for the final analysis.

The pathological features of the resected specimens were determined in accordance with the tumor node metastasis (TNM) system, based on the 8th edition of the Union for International Cancer Control (UICC) guidelines.[24] Perineural invasion was defined by the presence of cancer cells in the medial perineurium.

Follow-up examinations, including a computed tomography (CT) scan, were conducted every 3 months for the first 2 years and every 6 months thereafter. The median follow-up

period was 20.5 months (range, 3–113 months). New lesions detected using imaging were considered indicative of recurrence. Locoregional recurrence was defined as newly arising mass or lymph nodes around the pancreatic bed and the lympho-neural-dissected vessels. Distant metastasis was defined as lymph nodes apart from the pancreatic bed or tumor spread to liver, lung, and bone tissue. Peritoneal recurrence was defined as recurrence in the peritoneal cavity. This study was conducted in accordance with the declaration of Helsinki and approved by the Ethics Committee of the Hamamatsu University School of Medicine. Written informed consent was obtained from each patient.

Immunohistochemistry

Immunohistochemical staining for TNC, alpha smooth muscle actin (αSMA), glucose transporter 1 (Glut-1), and S-100 protein was performed using 4 μm-thick consecutive sections of formalin-fixed, paraffin-embedded (FFPE) tissues. The primary antibodies and dilutions used were follows: TNC, mouse monoclonal antibody (4F10TT, Immuno-Biological Laboratories, Gunma, Japan) at 1:6000; αSMA, mouse monoclonal antibody (M0851, Dako, Tokyo, Japan) at 1:200; Glut-1, rabbit polyclonal antibody (ab15309, Abcam, Tokyo, Japan) at 1:200; and S-100 protein, Rabbit Polyclonal Antibody (NCL-L-

S100p, Leica Biosystems, Newcastle, UK) at 1:1000. After deparaffinization and rehydration, samples were blocked with 3% hydrogen peroxide (H_2O_2) for 5 min at room temperature. Conditions for antigen retrieval were follows: TNC, incubation with Proteinase K (s302080, Dako) for 5 min at room temperature; and Glut-1, heating the samples at 96°C for 40 min in Tris/ ethylenediaminetetraacetic acid (EDTA) buffer (pH 9). Immunostaining of αSMA and S-100 protein did not require antigen retrieval. The samples were incubated overnight with the primary antibody for TNC and 30 min for the other proteins. The sections were washed and then incubated with the secondary antibody (K500711, Dako) for 30 min at room temperature. Staining signals were developed using 3,3′-diaminobenzidine (K500711, Dako). Counterstaining was performed with hematoxylin, followed by mounting.

Evaluation of TNC expression

All stained sections were scanned using an Aperio Digital Pathology Whole Slide Scanner (Leica Biosystems, Vista, Calif). Diagnosis was conducted in a virtual slide using an Aperio Image scope (Leica Biosystems). The invasive tumor front area was defined as the tumor periphery close to adjacent non-cancerous tissues such as the pancreas, adipose

tissue, or duodenum. To investigate the effect and distribution of TNC from the viewpoint of PNI, we evaluated TNC expression in fibrotic tissues around peripheral nerves (perineural sites) at the invasive tumor front. The TNC-staining intensity at perineural sites was scored as 0 (negative or obscure), 1 (weak), 2 (moderate), or 3 (strong) by comparison with that in adjacent non-cancerous tissues in the same section, according to the methods described by Murakami et al.[21] Smooth muscle and vessel wall staining intensities were considered as internal positive controls (Fig. S1), and normal duodenal mucosa was used as the negative control. We adopted the median score derived from at least five nerves randomly picked from the invasive tumor front, regardless of the presence of PNI. Three researchers (S.F., T.M., and M.F.), including one clinical pathologist, who were blinded to any clinical information independently evaluated TNC expression. When two or three researchers arrived at the same score, it was adopted as the final score. When three researchers obtained different score, the median score was adopted. TNC expression in perineural sites was finally classified as either low (0, 1) or high (2, 3, Fig. S2). Alpha smooth muscle actin expression in perineural sites at the invasive tumor front was also characterized as low (staining intensity less than that in cancer stroma) or high (greater than or equal to that in cancer stroma).

Cell culture

The human pancreatic cancer PANC-1 and MIA PaCa-2 cell lines, were purchased from RIKEN Bioresources Cell Bank (BRC Cell Bank, Ibaraki, Japan). The human pancreatic stellate cell line (HPSC) was purchased from Sciencell Research Laboratories (#3830, Carlsbad, Calif). PANC-1 cells were routinely grown in Roswell Park Memorial Institute (RPMI)-1640 (Wako, Osaka, Japan) supplemented with 10% fetal bovine serum (FBS) at 37ºC in a humidified atmosphere containing 5% CO_2. MIA PaCa-2 cells were grown in Dulbecco's modified Eagle's medium (DMEM, Invitrogen, Carlsbad, Calif) with 10% FBS at 37ºC in 5% CO_2 in a humid atmosphere. Human pancreatic stellate cells were grown with stellate cell medium (#5301, ScienCell Research Laboratories) at 2 μg/cm^2 in a poly-L-lysine-coated culture dish.

For Transwell co-cultures with HPSCs and PDAC cells, approximately 5 × 10^4 HPSCs were seeded into the lower chamber in a-6 well plate, with PDAC cells (5 × 10^4 PANC-1 cells or MIA PaCa-2 cells) growing in the top of the Transwell membrane (0.4 μm pore size, #3412, Corning Life Science, Tewksbury, Mass) (Fig. 6A). HPSCs co-cultured with PDAC cells for 2 days were used for assays and HPSCs in the monoculture were used as

controls.

Dorsal root ganglion separation and establishment of a cancer cell–nerve co-culture model

The following animal procedures were performed according to the guidelines of the Committee on Experimental Animals of Hamamatsu University School of Medicine. The methods used to isolate mouse DRGs were described by Ayala et al.[25] Neonatal (1-day-old) Institute of Cancer Research (ICR) mice (Japan SLC, Shizuoka, Japan) were anesthetized with isoflurane and euthanized by cervical dislocation. Each DRG was isolated by performing an anterior laminectomy and microscopic dissection from the lumbar spinal region. A single DRG was seeded on a 35 mm × 10 mm dish in a 5-μL drop of Matrigel (#356231, Matrigel® Growth Factor Reduced Basement Membrane Matrix, Corning, Inc., N.Y.), as the extracellular matrix. The dish was placed on ice to maintain the liquidity of the Matrigel.

The protocol used for establishing the cancer cell–DRG co-culture model was a modification of the method described by Li et al.[26] Briefly, 5×10^4 PDAC (PANC-1 or MIA PaCa-2) cells were suspended in a 5-μL Matrigel drop and placed approximately 1

mm away from the DRG suspension. To exclude the possibilities of unspecific cancer cell migration and neural outgrowth, an additional 5 μl "blank" Matrigel drop was positioned on the opposite side of each cell suspension (Fig. S3A). The dishes were then incubated at 37ºC with 5% CO_2 in a humid atmosphere for 20 min to allow for Matrigel polymerization. Each cell-suspended or blank Matrigel was connected via a 1 mm-long Matrigel plug, i.e., a "spacer" (Fig. S3A). After incubating for an additional 20 min in a humid atmosphere to polymerize the spacer, the Matrigels were carefully submersed in 2 mL of RPMI-1640 or DMEM supplemented with 2% FBS. To evaluate the molecular effects of TNC on cancer–neuron interactions *in vitro*, purified human TNC protein (CC065, Merck KGaA, Darmstadt, Germany) was mixed in the culture medium (TNC-CM, 1 μg/mL) or in the Matrigel (TNC-M, 10 μg/mL). The co-cultures were incubated at 37ºC with 5% CO_2 in a humid atmosphere for 4 days. Representative photographic documentation of the adjacent area of the two cell suspensions was performed using a microscope (Eclipse TE2000-U, Nikon, Tokyo, Japan) and an imaging system (AQUACOSMOS, Hamamatsu Photonics K.K, Shizuoka, Japan).

To quantitatively analyze the results of the co-culture model, we defined parameter γ as the minimum distance between the edge of PDAC cell-suspended Matrigel and the edge of

DRG, parameter α1 as the distance that cancer cells migrated towards the DRG, parameter α2 as the distance migrated away from the DRG, parameter β as the DRG outgrowth length towards cancer cells, the cancer invasion index as α1/γ, the DRG outgrowth index as β/γ, and the cancer neurotropic index as α1/α2 (Fig. S3B, C). Images of cancer cell migration and axonal outgrowth were captured and fused using a microscope (Biozero, KEYENCE, Osaka, Japan), and the distances were measured using ImageJ software (ImageJ 1.52a, Wayne Rasband, National Institutes of Health).[27]

We also investigated the axonal outgrowth of a single DRG with or without TNC supplementation. A single DRG was seeded on a 35 mm × 10 mm dish in a 5-μL drop of Matrigel and incubated for 20 min at 37ºC with 5% CO_2 in a humid atmosphere. Then, 2 mL RPMI-1640 or DMEM with 2% FBS was added, and the dish was incubated at 37ºC with 5% CO_2 in a humid atmosphere. The ratio of the area of axonal outgrowth to that of the DRG body was measured using ImageJ software 3 days after DRG suspension. Each experiment was performed at least 3 times independently, with 5 biological replicates.

Immunofluorescence staining

Double immunofluorescence staining of TNC and αSMA was performed using 4-μm-thick sections of FFPE tissues to examine the cellular localization of each protein marker. After deparaffinization and antigen retrieval as described above, the samples were blocked in 3% normal chicken serum for 20 min. Next, the sections were incubated overnight with the following primary antibodies: TNC, mouse monoclonal antibody (4F10TT, Immuno-Biological Laboratories) at 1:500; αSMA, rabbit polyclonal antibody (ab5694, Abcam) at 1:200. On the next day, the sections were incubated with the following secondary antibodies: chicken anti-mouse IgG antibody conjugated Alexa Fluor 594 (A-21201, Life Technologies, Carlsbad, Calif) at 1:200, anti-rabbit IgG conjugated Alexa Fluor 488 (A-21441, Life Technologies) at 1:200. Additional nuclear staining was performed using the ProLong Gold Antifade reagent with 4',6-diamidino-2-phenylindole (DAPI, P36935, Life Technologies). Immunofluorescence imaging was performed using the confocal microscope (Photometrics Evolve 512, Nippon Roper, Tokyo, Japan) and image analysis system (Lumina Vision version 3.0, Mitani Corp., Tokyo, Japan).

For immunofluorescence staining of PDAC cell lines , the above-mentioned *in vitro* PDAC cell (PANC-1, MIA PaCa-2)-nerve co-culture model was incubated on an 18 × 18 mm round cover glass in a 6-well plate for 4 days. The dish was washed with phosphate-

buffered saline (PBS), fixed with 4% paraformaldehyde for 30 min, and blocked with 5% normal chicken serum with 0.1% Triton X (T8787, Sigma-Aldrich, St. Louis, Mo) for 1 h. The samples were then incubated overnight with the following primary antibodies: E-cadherin, rabbit polyclonal antibody (HPA004812, Sigma-Aldrich) at 1:200; vimentin, mouse monoclonal antibody (ab8978, Abcam) at 1:500. The secondary antibody and additional nuclear staining were conducted as described above. Imaging procedures were performed using an SP8 Confocal inverted microscope (Leica Microsystems, Tokyo, Japan) and image analysis system (Leica Application Suite X, Leica Microsystems).

Cell-proliferation assay

Cell proliferation was evaluated by counting the number of viable cells, as reported previously.[28] PANC-1 or MIA PaCa-2 cells (estimated 3,000 cells) were cultured in 96-well plates with RPMI-1640 medium or DMEM containing 2% FBS and incubated at 37ºC saturated with 5% CO_2 in a humid atmosphere, respectively. After 24 h, the medium was removed and 100 μL of RPMI-1640 medium or DMEM with 2% FBS and 1 or 5 μg/mL TNC was added to each well. Cell proliferation was measured 3 days after changing the medium. The cells were washed with PBS, fixed with 4% paraformaldehyde for 30 min,

and stained with DAPI solution (340-07971, Wako) for 3 min. The cells were imaged using an automated microscope (IN Cell Analyzer 2200, GE Healthcare, Little Chalfont, UK). Cell counting was performed using IN Cell Investigator software (GE Healthcare). The analysis was performed on 10 independent wells for each condition.

RNA extraction and quantitative RT-PCR

Total RNA from HPSCs in monoculture or co-cultured with PDAC cells was extracted with an RNAeasy Mini kit (Qiagen, Hilden, Germany) according to the manufacturer's protocol. The quality and quantity of the total RNA were evaluated using a NanoDrop1000 spectrophotometer (NanoDrop Technologies, Wilmington, Del). Reverse transcription was performed using the Primer script RT Reagent kit (Takara Bio, Otsu, Japan). cDNA was amplified by quantitative RT-PCR (qRT-PCR) on a thermal Cycler Dice Real Time System II (Takara Bio) using Thunderbird 1PCR Mix (Toyobo Life Science, Osaka, Japan). All PCRs were performed in at least triplicate, and the relative levels of genes normalized to the control were calculated using 2nd derivative maximum methods. The sequences of primers used for amplification were as follows: 5′-CTCCCAGTGACAACATCGCAATA-3′ and 5′-GGATGGCTTCCAATGACACATTTA-3′ for *TENASCIN C*; 5′-

ATTGCCGACCGAATGCAGA-3′ and 5′-ATGGAGCCACCGATCCAGAC-3′; *αSMA*, 5′-TGGCACCCAGCACAATGAA-3′ and 5′-CTAAGTCATAGTCCGCCTAGAAGCA-3′; *β-ACTIN*. mRNA levels were normalized to *β-actin*.

Western blotting

The procedures were previously described.[21] Cells were lysed in chilled lysis buffer supplemented with complete protease and phosphatase inhibitor cocktail (Roche, Basel, Switzerland). Protein concentrations were determined using a Bicinchoninic Acid Protein Assay Kit (Takara Bio). The whole cell lysates (30-60 μg) were subjected to polyacrylamide- sodium dodecyl sulfate gradient gel (Kanto Chemical, Tokyo, Japan) electrophoresis followed by electroblotting onto an Immobilon-Polyvinylidene fluoride membrane (Millipore, Billerica, Mass). After blocking with 3% skim milk for 1 h, the membranes were incubated at 4°C overnight with the following primary antibodies: Tenascin C, mouse monoclonal antibody (4F10TT, Immuno-Biological Laboratories) at 1:500; αSMA, mouse monoclonal antibody (M0851, Dako) at 1:500; β-actin (#5125, Cell Signaling Technology, Danvers, Mass) at 1:1000. On the next day, the membrane was incubated for 1 h at room temperature with horseradish peroxidase-conjugated secondary

antibodies. Primary and secondary antibodies were diluted in Can Get Signal Immunoreaction Enhancer Solution (Toyobo Life Science). Immunoreactive bands were visualized using Enhanced Chemiluminescence Plus Western Blotting Detection Reagent (GE Healthcare) and a FUSION SYSTEM (Vilber-Lourmat, Collégien, France).

Statistical analysis

Student's *t*-test, the χ^2 test, and Fisher's exact test were used for univariate analysis to evaluate the associations between TNC expression and clinicopathological features. The Kaplan–Meier method and log-rank test were used to estimate postoperative prognosis. The Cox proportional hazard model was used to evaluate the hazard ratio for each variable in univariate and multivariate analyses. The *in vitro* data were analyzed using Student's *t*-test. *P*-values < 0.05 were considered statistically significant. All calculations were performed using the statistical package for the social sciences (SPSS) 24.0 software (SPSS, Inc., Chicago, Ill).

Results

Immunohistochemical detection of TNC expression in PDACs

Tenascin C was expressed mainly in cancer stromal tissue. Adjacent normal tissues showed very weak or no TNC expression, except for smooth muscles and vessel walls. Few cancer cells showed cytoplasmic or membranous TNC staining.

At the invasive tumor front, TNC expression was predominantly observed in perineural sites (Fig. 1A, B), whereas TNC expression was not observed in perineural sites with adjacent non-cancerous (Fig. 1C) areas. Alpha smooth muscle actin showed a similar staining pattern as TNC (Fig. 1D). Furthermore, rim-like TNC staining overlapped with staining for Glut-1, a perineurium marker,[29] but not S-100 protein, a peripheral nerve marker (Fig. 1E, F). Double immunofluorescences staining for TNC and αSMA showed that TNC was expressed close to αSMA-positive spindle-shape like cells (Fig. 1G–J).

Relationships between TNC expression in perineural sites and clinicopathological features

Based on our classification of TNC expression in perineural sites as being either low or high (Fig. S2), we found that 48 (62%) and 30 (38%) patients with PDAC showed low and

high TNC expression, respectively in perineural sites at the invasive tumor front. The detailed patient characteristics are shown in Table 1. High TNC expression was significantly associated with the presence of PNI ($P = 0.008$) and pathological T stage (pT) ≥ 3 ($P = 0.021$). The αSMA and TNC staining patterns were also significantly correlated ($p < 0.001$).

Next, we analyzed the effect of TNC expression in perineural sites on postoperative prognosis. Kaplan–Meier analysis revealed that patients with high TNC expression had significantly shorter recurrence-free survival ($p < 0.001$, Fig. 2A) and overall survival ($P = 0.009$, Fig. 2B). Univariate analysis revealed that recurrence-free survival correlated with carbohydrate antigen 19-9 (CA 19-9) ≥ 77 ($P = 0.014$), the G3 histological type ($P = 0.003$), the presence of lymphatic invasion ($P = 0.002$), the presence of PNI ($p < 0.001$), pT ≥ 3 ($P = 0.023$), the presence of lymph node metastasis ($P = 0.002$), pStage ≥ IIB ($P = 0.001$), microscopic residual tumor (R1 resection, $P = 0.024$), high TNC expression ($P = 0.001$), and high αSMA expression ($P = 0.022$), as shown in Table 2. Multivariate analyses revealed that the Grade 3 histological type (G3, $P = 0.011$), the presence of PNI ($P = 0.001$), and high TNC expression ($P = 0.045$) were independent poor prognostic factors (Table 2). Regarding overall survival, multivariate analyses showed that the presence of

PNI was a poor prognostic factor ($P = 0.009$, data not shown), while TNC expression in perineural sites was not ($P = 0.124$, data not shown).

Relationships between TNC expression in perineural sites and recurrence pattern

In 78 patients with PDAC, 66 postoperative recurrences were identified in 53 patients during the study period. Categorizing the recurrence pattern into locoregional, distant, and peritoneal sites showed that locoregional recurrence significantly increased in patients with high TNC expression in perineural sites ($P = 0.002$, Table 3).

Tenascin C enhanced cancer cell–nerve interactions in an* in vitro *co-culture model

Next, we assessed the molecular effects of TNC using an *in vitro* co-culture model with PDAC cells and a DRG. The extensions of PANC-1 cell colonies and DRG outgrowth were not affected by TNC supplementation in the culture medium (TNC-CM, Fig. 3A, B, D, and E). Surprisingly, with TNC supplementation in the Matrigel (TNC-M), PANC-1 cell colonies extended toward the DRG with spike formations, and DRG axonal fibers grew toward cancer cells (Fig. 3C, F and H). Furthermore, more extensions of cancer cell colonies were observed in the adjacent area of the DRG than on the opposite side of the

DRG (Fig. 3F, G). Quantitative analysis showed that the cancer invasion index, DRG outgrowth index, and cancer neurotropic index values increased significantly in the co-culture model with TNC-M, compared to those with control treatment or TNC-CM (Fig. 3I–K). Similar results were obtained with another PDAC cell line, MIA PaCa-2 (Fig. 3L–V).

Tenascin C did not affect axonal outgrowth of DRG or PDAC cell proliferation in monocultures

To investigate the direct effects of TNC on DRG cells or PDAC cells, DRGs were grown in monoculture with TNC-CM or TNC-M. Axonal outgrowth of single DRGs was not promoted by TNC supplementation, compared to control treatment (Fig. 4A, B). Furthermore, the proliferation of PDAC cells did not significantly increase when cells were cultured in the presence of TNC-CM (Fig. 4C, D).

Vimentin expression was observed in PDAC cells adjacent to DRG with TNC supplementation in Matrigel

To investigate the molecular modulation of PDAC cells in the co-culture model with TNC

supplementation in Matrigel, such as epithelial-mesenchymal-transition (EMT), expression of classical EMT markers in PDAC cells was assessed. Immunofluorescence study showed that PDAC cells adjacent to DRG were mostly composed of E-cadherin-predominant cells in the control or TNC-CM co-culture model (Fig. 5A, B, E, F). Interestingly, spindle-shaped PDAC cells at the extended front of the adjacent area showed high vimentin expression in the TNC-M model (Fig. 5C, G), whereas those in the opposite area did not (Fig. 5D, H). The protein levels of E-cadherin and vimentin in PDAC cells collected from whole cell colonies in the co-culture model were not significantly different following TNC supplementation (western blotting analysis, data not shown).

Pancreatic stellate cells co-cultured with PDAC cells induced Tenascin C expression

Additionally, we investigated the role of PSCs, which are major components of the extracellular matrix in PDAC. The levels of mRNA were upregulated in HPSCs co-cultured with PDAC cells (PANC-1, MIA PaCa-2) in the Transwell system compared to those in monoculture (Fig. 6B). In contrast, the protein expression of TNC was not increased in HPSCs with or without co-culture with PDAC cells (Fig. 6D). We also confirmed upregulated mRNA and protein expression of αSMA in HPSCs co-cultured with PDAC

cells (Fig. 6C, D).

Discussion

Discovering the mechanisms that promote PNI in PDAC is important for identifying target molecules for diagnosis or therapy of this dismal disease, and may contribute to relieving cancer-related refractory pain in patients who are suffering. Although direct tumor–nerve interactions have been previously discussed in terms of the mechanisms of PNI,[13] the roles of the surrounding tumor–nerve microenvironment are less studied. In this regard, focusing on extracellular matrix proteins (including TNC) in the tumor–nerve microenvironment may lead to novel breakthroughs in understanding the mechanisms of PNI.

In this study, we sought to clarify the roles of TNC in PNI of PDAC for the first time. Immunohistochemical examination of resected PDAC specimens showed that TNC expression occurred predominantly in perineural sites at the invasive tumor front, but was not observed in adjacent non-cancerous areas. Interestingly, TNC overexpression in perineural sites overlapped with the perineurium and was associated with strong αSMA expression. Furthermore, TNC expression was located close to αSMA-positive cells, as shown in Fig. 1H–J. These results indicate that TNC is abundant in tumor-nerve microenvironment and would derive from an active phenotype of fibroblasts that configures

the perineurium. The perineurium–Henle layer was originally described as a sheath of vitreous-to-hyaline material surrounding nerve fascicles.[30] The perineurium is composed of perineural cells, which do not have a neural crest cell origin, but are derived from mesenchymal cells, that is, fibroblasts, which surround adjacent nerve fibers.[31,32] The perineurium maintains a constant intrafascicular pressure and guarantees a selective barrier effect for the axons and Schwann cells.[33,34]

In the peripheral nervous system, TNC is diffusely expressed during neurogenesis, however, its expression is lost or reduced after birth.[35] Tenascin C expression reappears under pathological conditions including inflammation, tumorigenesis, and regeneration following injury in developed organs.[15,16] Recently, several studies have shown that TNC is constitutively expressed in perineural cells.[36 37] Yamamoto et al [38] reported that TNC mediates regeneration of the perineurium after microsurgical resection in an *in vivo* model. Based on our results and those of previous studies, we speculated that once the perineurium is involved or contacts cancer cells, perineural cells acquire the activated phenotype (i.e., cancer-associated fibroblasts) and then secrete TNC, which helps regenerate injured nerves and unexpectedly attracts cancer cells to the perineural niche by conferring migration and invasion abilities.

We also investigated the roles of PSCs, which are major components in the extracellular matrix in the tumor-nerve microenvironment. As shown in Fig. 6, the mRNA level of TNC was increased in HPSCs co-cultured with PDAC cells compared to those in monoculture. The unchanged protein level of TNC in HPSCs would reflect that TNC is secreted into the extracellular space and exerts its effect soon after its production in HPSCs. These observations agree with those of previous studies showing that PSCs, activated by cancer cells, are important sources of TNC.[22] This also supports our hypothesis that αSMA-positive cells, such as perineural cells and PSCs, in the tumor-nerve microenvironment can produce TNC and contribute to PNI.

In terms of the relationships between TNC expression and clinicopathological factors, this present study revealed that strong TNC expression in perineural sites at the invasive front of PDAC significantly correlated with the presence of PNI and poor prognosis, with locoregional recurrence. Furthermore, strong TNC expression in perineural sites was indicated as an independent poor prognostic factor for recurrence-free survival. However, we noted that some cases did not show a coincidence of PNI and high TNC expression as shown in Table 1. This clinical discrepancy may reflect difficulties in the histological evaluation of PNI. We frequently encounter a diagnostic dilemma in terms of the definition,

extent, and severity of histological PNI from resected specimens. Chi et al [39] pointed out that interobserver variations exist among pathologists in evaluating histological PNI because the proposed definitions of PNI vary considerably, as determine by the locational relationships between tumor cells and nerve sheath layers. In our study, among 54 patients histologically diagnosed with PNI, those with high TNC expression tended to have a poorer prognosis for recurrence-free survival than those with low TNC expression did ($P = 0.122$, log-rank test, Fig. S4). Furthermore, all four patients with high TNC expression who did not show histological PNI experienced recurrence (median time to recurrence: 32 months; range, 7-43), including three cases (75%) as with locoregional recurrence. Assuming that perineural TNC expression results from the contact or involvement of cancer cells in the perineurium that leads to PNI, immunohistochemical TNC staining may be helpful not only as an objective diagnostic biomarker for confirming PNI, but also as a potential indicator for occult PNI in cases without any obvious evidence of histological PNI.

In the present *in vitro* co-culture experiments, we found that TNC in Matrigel significantly enhanced both polarized neurotropic migration of cancer cells and axonal outgrowth of nerves toward cancer cells. Interestingly, cancer cell–nerve interactions were not enhanced by supplementing the medium with TNC. Furthermore, TNC supplementation did not

significantly enhance DRG outgrowth or PDAC cell proliferation when these cell types were grown separately. These findings indicate that TNC exerts its molecular function as a transit signal during cancer cell–nerve interactions in both cancer cells and nerves only when it is abundant in the extracellular matrix as a scaffold protein in the tumor–nerve microenvironment, which closely resembles the *in vivo* situation.

It has been reported that cancer cells and nerves are mutually attracted to each other due to paracrine signaling. Previous findings showed that the attraction of nerve fibers is mediated by the production of neurotrophic growth factors by cancer cells.[40] Furthermore, Gil et al [41] reported that polarized neurotropic migration of cancer cells was induced by glial cell-derived neurotrophic factor secretion from nerves. Recently, PSCs, inflammatory cells, and Schwann cells (which configure the tumor–nerve microenvironment) were reported to help promote cancer cell–nerve interactions, resulting in PNI.[26,42]

Tenascin C has a mass of approximately 300 kDa and contains four individual domains.[43] Multiple cell surface TNC receptors have been identified, and each TNC domain binds a different receptor for a distinct function.[43] In pancreatic cancer, Annexin A2 is known to function as a receptor for TNC [22]. Annexin A2 binds the fibronectin type III domain of TNC, disassembling focal adhesion and actin stress fibers to promote cell detachment and

motility.[44] In the peripheral nervous system, various receptors for TNC such as integrin αvβ3, α9β1, and Annexin A2 may be involved in the differentiation and proliferation of neural precursor cells, or regeneration by neurite outgrowth after nerve injury.[45] Regarding TNC localization, Paron et al [23] showed that a TNC-rich matrix increased pancreatic cancer cell migration while TNC in the culture medium did not, and reported that the pleiotropic effects of TNC depended on the cellular and tissue context. These reports support the speculation based on our present results that a TNC-rich tumor–nerve microenvironment may enhance mutual tropisms.

In this study, we found altered EMT-related markers in extended spindle-shape PDAC cells adjacent to DRG in the *in vitro* co-culture model with TNC supplementation in Matrigel (Fig. 5). In contrast, the protein levels of EMT markers in PDAC cells collected from whole cell colonies in the co-culture model were not changed. This indicates that Tenascin C can enhance the invasion abilities of PDAC cells toward nerves by driving EMT; however, this effect appears to be limited to the adjacent area via interactions between PDAC cells and nerves. It is widely known that EMT plays a major role in tumor progression.[46] Tumor cells can acquire a mesenchymal phenotype by triggering the intrinsic cellular program of EMT to promote cell invasiveness. Regarding the relationship between

EMT and TNC, Nagaharu et al reported that TNC induces EMT-like changes accompanied by SRC activation and focal adhesion kinase phosphorylation in human breast cancer cells.[47] Furthermore, Zhang et al reported that macrophage migration inhibitory factor promotes perineural invasion through EMT in salivary adenoid cystic carcinoma.[48] These reports appear to support our suggestion that TNC enhances the interaction between tumor cells and nerve, altering PDAC cells to undergo EMT programming.

Our study has some limitations. First, immunohistochemical analyses were performed retrospectively with a relatively small number of patients; thus, a prospective study with a larger sample size is required for further confirmation. Second, we did not elucidate the detail TNC-mediated signaling pathway in PDAC cells that leads to EMT-associated perineural invasion. Further investigations of TNC receptors and downstream signaling molecules that drive mutual tropisms are warranted.

Furthermore, we utilized human-derived PDAC cells and mouse-derived neural cells in the *in vitro* co-culture model. This model has advantages for evaluating both the neurotropism of cancer cells and tumor tropism of neural cells by placing each cell type separately in Matrigel and determining the development of perineural invasion by cancer-neuron contact in a time-dependent manner. Additionally, this model enables investigation

of the modulation of paracrine signaling by controlling the extracellular matrix conditions such as by adding chemoattractants or proteins such as TNC to the Matrigel. This co-culture model has been widely accepted to mimic the situation of perineural invasion *in vivo* and as described in various studies.[13,25,26,41] Further studies are needed to establish a co-culture model using human-derived neural cells to more closely resemble the *in vivo* situation. Additionally, *in vivo* experiments such as orthotopic transplantation of PDAC cell with/without TNC in immunodeficient mice or using PDAC model mice is needed to support our hypothesis.

In conclusion, we demonstrated the functional role of TNC in PNI of PDAC. These findings suggest that TNC could be targeted to reduce PNI and improve the survival of patients with PDAC.

Acknowledgments:

We thank Dr Masaki Sano, Yuki Kurita, and Yayoi Kawabata for their expert technical advice.

Disclosure Statement:

The authors have no conflict of interest to declare.

References:

1. Siegel RL, Miller KD, Jemal A. Cancer statistics. 2016. *CA Cancer J Clin*. 2016;66:7-30.

2. Greer JB, Brand RE. New developments in pancreatic cancer. *Current Gastroenterol Rep*. 2011;13:131-139.

3. Oettle H. Progress in the knowledge and treatment of advanced pancreatic cancer: from benchside to bedside. *Cancer Treat Rev*. 2014;40:1039-1047.

4. Hirai I, Kimura W, Ozawa K, et al. Perineural invasion in pancreatic cancer. *Pancreas*. 2002;24:15-25.

5. Barbier L, Turrini O, Gregoire E, et al. Pancreatic head resectable adenocarcinoma: preoperative chemoradiation improves local control but does not affect survival. *HPB*. 2011;13:64-69.

6. Ben QW, Wang JC, Liu J, et al. Positive Expression of L1-CAM is associated with perineural invasion and poor outcome in pancreatic ductal adenocarcinoma. *Ann Surg Oncol*. 2010;17:2213-2221.

7. Ceyhan GO, Bergmann F, Kadihasanoglu M, et al. Pancreatic neuropathy and neuropathic pain–a comprehensive pathomorphological study of 546 cases.

Gastroenterology. 2009;136:177-186.e171.

8. Lenz J, Karasek P, Jarkovsky J, et al. Clinicopathological correlations of nestin expression in surgically resectable pancreatic cancer including an analysis of perineural invasion. *J Gastrointestin Liver Dis.* 2011;20:389-396.

9. Chatterjee D, Katz MH, Rashid A, et al. Perineural and intraneural invasion in posttherapy pancreaticoduodenectomy specimens predicts poor prognosis in patients with pancreatic ductal adenocarcinoma. *Am J Surg Pathol*. 2012;36:409-417.

10. Badger SA, Brant JL, Jones C, et al. The role of surgery for pancreatic cancer: a 12-year review of patient outcome. *Ulster Med J*. 2010;79:70-75.

11. Zhu Z, Friess H, diMola FF, et al. Nerve growth factor expression correlates with perineural invasion and pain in human pancreatic cancer. *J Clin Oncol*. 1999;17:2419-2428.

12. Bockman DE, Buchler M, Beger HG. Interaction of pancreatic ductal carcinoma with nerves leads to nerve damage. *Gastroenterology*. 1994;107:219-230.

13. Liebig C, Ayala G, Wilks JA, et al. Perineural invasion in cancer: a review of the literature. *Cancer*. 2009;115;3379-3391.

14. Tucker RP, Chiquet-Ehrismann R. The regulation of tenascin expression by tissue

microenvironments. *Biochim Biophys Acta*. 2009;1793:888-892.

15. Jones FS, Jones PL. The tenascin family of ECM glycoproteins: structure, function, and regulation during embryonic development and tissue remodeling. *Dev Dyn*. 2000;218:235-259.

16. Chiquet-Ehrismann R, Chiquet M. Tenascins: regulation and putative functions during pathological stress. *J Pathol*. 2003;200:488-499.

17. Chiquet-Ehrismann R, Mackie EJ, Pearson CA, et al. Tenascin: an extracellular matrix protein involved in tissue interactions during fetal development and oncogenesis. *Cell*. 1986;47:131-139.

18. Aishima S, Taguchi K, Terashi T, et al. Tenascin expression at the invasive front is associated with poor prognosis in intrahepatic cholangiocarcinoma. *Mod Pathol*. 2003;16:1019-1027.

19. Herold-Mende C, Mueller MM, Bonsanto MM, et al. Clinical impact and functional aspects of tenascin-C expression during glioma progression. *Int J Cancer*. 2002;98:362-369.

20. Jahkola T, Toivonen T, Virtanen I, et al. Tenascin-C expression in invasion border of early breast cancer: a predictor of local and distant recurrence. *Br J Cancer*.

1998;78:1507-1513.

21. Murakami T, Kikuchi H, Ishimatsu H, et al. Tenascin C in colorectal cancer stroma is a predictive marker for liver metastasis and is a potent target of miR-198 as identified by microRNA analysis. *Br J Cancer*. 2017;117:1360-1370.

22. Esposito I, Penzel R, Chaib-Harrireche M, et al. Tenascin C and annexin II expression in the process of pancreatic carcinogenesis. *J Pathol*. 2006;208:673-685.

23. Paron I, Berchtold S, Voros J, et al. Tenascin-C enhances pancreatic cancer cell growth and motility and affects cell adhesion through activation of the integrin pathway. *PLoS One*. 2011;6:e21684.

24. Brierley J, Gospodarowicz M, Wittekind C. Union For International Cancer Control. *TNM Classification of Malignant Tumours, Eighth Edition.* Chichester: Wiley-Blackwell, 2017.

25. Ayala GE, Wheeler TM, Shine HD, et al. In vitro dorsal root ganglia and human prostate cell line interaction: redefining perineural invasion in prostate cancer. *Prostate*. 2001;49:213-223.

26. Li X, Wang Z, Ma Q, et al. Sonic hedgehog paracrine signaling activates stromal cells to promote perineural invasion in pancreatic cancer. *Clin Cancer Res*. 2014;20:4326-

4338.

27. Rasband WS. ImageJ, U. S. National Institutes of Health, Bethesda, Maryland, USA, https://imagej.nih.gov/ij/, 1997-2018.

28. Takeda M, Sakaguchi T, Hiraide T, et al. Role of caveolin-1 in hepatocellular carcinoma arising from non-alcoholic fatty liver disease. *Cancer Sci*. 2018;109:2401-2411.

29. Pina AR, Martinez MM, de Almeida OP. Glut-1, best immunohistochemical marker for perineurial cells. *Head Neck Pathol*. 2015;9:104-106.

30. Thomas PK, Ochoa J. Microscopic Anatomy of Peripheral Nerve Fibers. In: Dick PJ, Thomas PK, Lambert EH, et al, eds. *Peripheral Neuropathy*. Philadelphia: Saunders, 1984;1:39-96.

31. Joseph NM, Mukouyama YS, Mosher JT, et al. Neural crest stem cells undergo multilineage differentiation in developing peripheral nerves to generate endoneurial fibroblasts in addition to Schwann cells. *Development*. 2004;131:5599-5612.

32. Rosenbaum T, Boissy YL, Kombrinck K, et al. Neurofibromin-deficient fibroblasts fail to form perineurium in vitro. *Development.* 1995;121:3583-3592.

33. Rechthand E, Smith Q, Rapoport S. A compartmental analysis of solute transfer and

exchange across blood-nerve barrier. *Am J Physiol*. 1988;255:R317-R325.

34. Thomas E, Sourander P. Impaired development of the rat perineurium by undernutrition. *Acta Neuropathol*. 1977;38:77-80.

35. Chiquet M, Fambrough DM. Chick myotendinous antigen. I. A monoclonal antibody as a marker for tendon and muscle morphogenesis. *J Cell Biol*. 1984;98:1926-1936.

36. Nishimura T, Hirata H, Tsujii M, et al. Pathomechanism of entrapment neuropathy in diabetic and nondiabetic rats reared in wire cages. *Histol Histopathol*. 2008;23:157-166.

37. Hill R. Extracellular matrix remodelling in human diabetic neuropathy. *J Anat*. 2009;214:219-225.

38. Yamamoto M, Okui N, Tatebe M, et al. Regeneration of the perineurium after microsurgical resection examined with immunolabeling for tenascin-C and alpha smooth muscle actin. *J Anat*. 2011;218:413-425.

39. Chi AC, Katabi N, Chen HS, et al. Interobserver variation among pathologists in evaluating perineural invasion for oral squamous cell carcinoma. *Head Neck Pathol*. 2016;10:451-464.

40. Magnon C, Hall SJ, Lin J, et al. Autonomic nerve development contributes to prostate cancer progression. *Science*. 2013;341:1236361.

41. Gil Z, Cavel O, Kelly K, et al. Paracrine regulation of pancreatic cancer cell invasion by peripheral nerves. *J Natl Cancer Inst*. 2010;102:107-118.

42. Na'ara S, Amit M, Gil Z. L1CAM induces perineural invasion of pancreas cancer cells by upregulation of metalloproteinase expression. *Oncogene*. 2018;38:596-608.

43. Lowy CM, Oskarsson T. Tenascin C in metastasis: a view from the invasive front. *Cell Adh Mig*. 2015;9:112-124.

44. Murphy-Ullrich JE, Lightner VA, Aukhil I, et al. Focal adhesion integrity is downregulated by the alternatively spliced domain of human tenascin. *J Cell Biol*. 1991;115:1127-1136.

45. Garcion E, Faissner A, ffrench-Constant C. Knockout mice reveal a contribution of the extracellular matrix molecule tenascin-C to neural precursor proliferation and migration. *Development*. 2001;128:2485-2496.

46. Brabletz T, Kalluri R, Nieto Ma, et al. EMT in cancer. *Nat Rev Cancer.* 2018;18:128-134.

47. Nagaharu K, Zhang X, Yoshida T, et al. Tenascin C induces epithelial-mesenchymal transition-like change accompanied by SRC activation and focal adhesion kinase phosphorylation in human breast cancer cells. *Am J Pathol.* 2011;178:754-763.

48. Zhang M, Li ZF, Wang HF, et al. MIF promotes perineural invasion through EMT in salivary adenoid cystic carcinoma. *Mol Carcinog.* 2019;58:898-912.

Figure legends:

Figure 1. (A) Representative images of tenascin C (TNC) immunostaining in resected pancreatic ductal adenocarcinoma (PDAC) tissues. Red dotted line indicates border between invasive front of PDAC and adjacent non-cancerous tissue. As shown in magnified views, TNC was (B) overexpressed in perineural sites at invasive front, whereas its expression was (C) absent in non-cancerous areas. Immunostaining of (D) αSMA, (E) Glut-1, and (F) S-100 protein in consecutive sections of same specimens (Ca: cancer, Non-Ca: non-cancer, N: nerve, black scale bar: 100 μm, white scale bar: 20 μm). (G) Tenascin C immunostaining at the perineural site with perineural invasion. In magnified views of the red box area in (G), representative immunofluorescence images of (H) TNC (green), (I) αSMA (magenta), (H, I) DAPI nuclear counterstaining (blue), and (J) merge are shown. Tenascin C expression was closely located around αSMA-positive spindle-shape cells (arrowheads). (N: nerve, T: tumor cells, black scale bar: 100 μm, white scale bar: 20 μm).

Figure 2. Kaplan–Meier survival curves of (A) recurrence-free survival and (B) overall survival of patients with pancreatic ductal adenocarcinoma (PDAC), stratified by tenascin C (TNC) expression pattern in perineural sites.

Figure 3. *In vitro* pancreatic ductal adenocarcinoma (PDAC) cell–dorsal root ganglion (DRG) co-culture model using PANC-1 (A–K) or MIA PaCa-2 (L–V) cell line, respectively. (A, L) Representative microphotographs after 4-day treatment with vehicle control, (B, M) tenascin C-supplemented culture medium (TNC-CM) (1 μg/mL in culture medium), and (C, N) tenascin C in Matrigel (TNC-M) (10 μg/mL in Matrigel). Yellow and purple dotted lines show edges of outgrowing DRG neurites and pancreatic cell colonies, respectively. Red, dotted straight line shows minimum distance between edge of PDAC cells suspended in Matrigel and that of a DRG (γ). (D–F and O–Q) Magnified views of adjacent areas of two cell suspensions (black dotted boxes in panels A–C and L–M, respectively). (G and R) Magnified views of the opposite side of pancreatic cell colonies in C and N (in blue dotted box), respectively. (H and S) Magnified views of cells in orange dotted box in F and Q, respectively. White arrowheads indicate contacts between DRG axonal fibers and cancer cell colonies with spike formations. (black bars in A–C and L–M: 500 μm, white bars in D–G and O–Q: 300 μm, orange bars in H and S: 100 μm, *: $P < 0.05$, **: $P < 0.01$)

Figure 4. Representative photographic images of axonal outgrowth of single dorsal root ganglion (DRG) on day 3 with tenascin C-supplemented culture medium (TNC-CM, 1 μg/mL purified human TNC protein mixed in culture medium) or TNC-M (10 μg/mL purified human TNC protein mixed in Matrigel) (A). Yellow dotted line shows edge of axonal outgrowth and red dotted line shows DRG body outline. Ratio of axonal outgrowth of DRG with TNC-CM (1 μg/mL) or TNC-M (10 μg/mL) (B). (C, D) Pancreatic ductal adenocarcinoma (PDAC) cell proliferation (C: PANC-1, D: MIA PaCa-2) in TNC-CM (1 or 5 μg/mL). Cell-proliferation ratio was evaluated 3 days after changing the medium.

Figure 5. Immunofluorescence staining of E-cadherin (green) and vimentin (magenta) in *in vitro* pancreatic ductal adenocarcinoma (PDAC) cell–dorsal root ganglion (DRG) co-culture model using PANC-1 (A–D) and MIA PaCa-2 (E–H) cells. Representative micrographs of magnified views of red box at the adjacent area and opposite area are shown. Spindle-shape PDAC cells at the adjacent area in Tenascin C in the Matrigel (TNC-M) model were rich with vimentin expressions (arrow head). (TNC-CM: Tenascin C in the culture medium, white bars: 300 μm, yellow bars: 50 μm).

Figure. 6 Schemas of human pancreatic stellated cells co-cultured with human PDAC cell lines using Transwell chamber model (A). Quantitative RT-PCR (B) and western blotting analyses (C) of Tenascin C and αSMA expression in HPSCs monocultured or co-cultured with PDAC cells (PANC-1, MIA PaCa-2) (*: $P < 0.05$).

Supplemental Data File

Figure S1. Immunohistochemical staining of Tenascin C (TNC) for smooth muscle and vessel wall as internal positive control in PDAC specimens

Figure S2. Representative immunostaining of tenascin C (TNC) in perineural sites

Figure S3. Illustrations of in vitro co-culture model

Figure S4. Kaplan-Meier survival curves of recurrence-free survival of patients with perineural invasion (n = 54)

Fig. 1

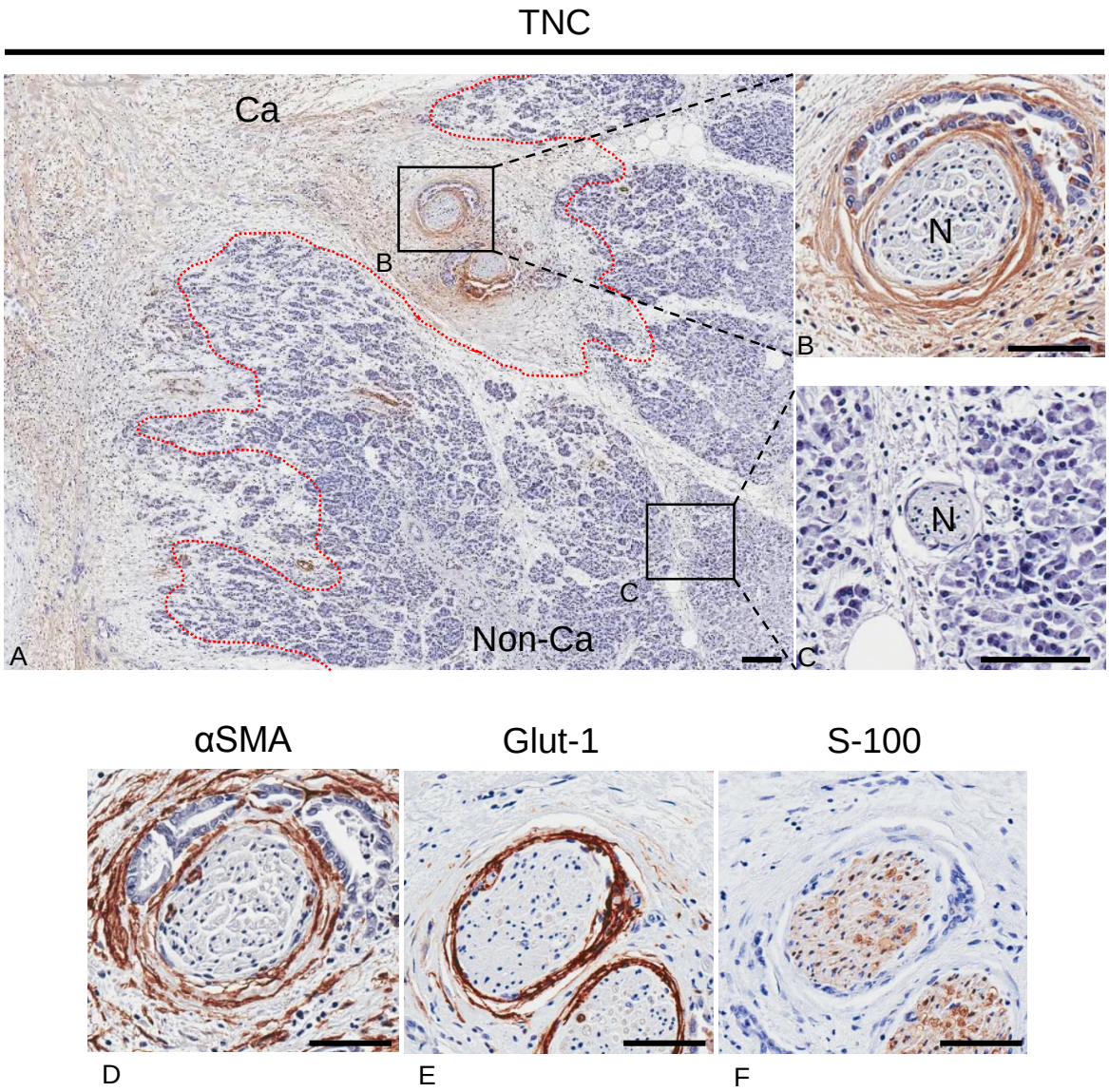

TNC

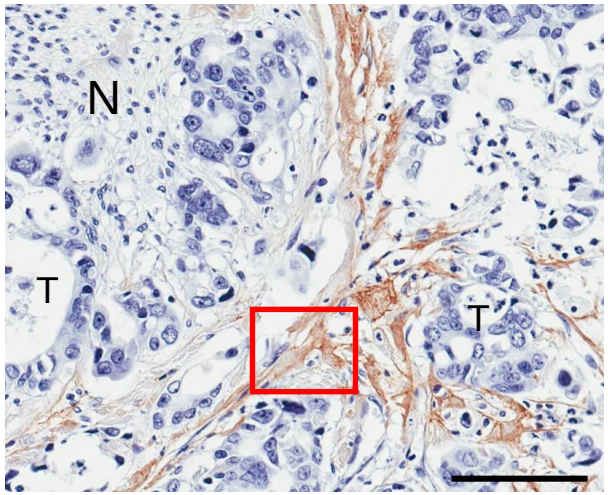

G

TNC / DAPI

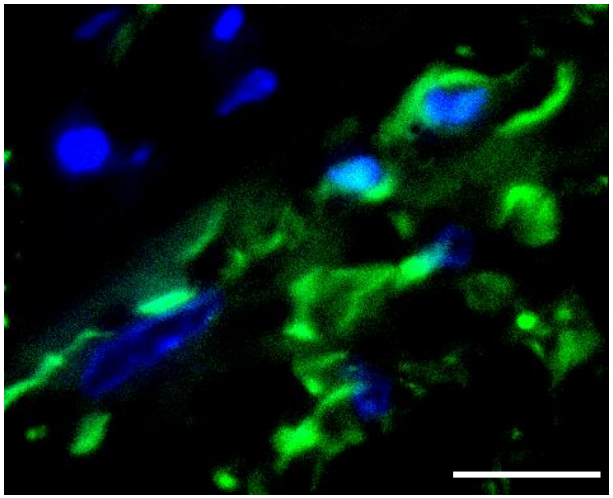

H

αSMA / DAPI

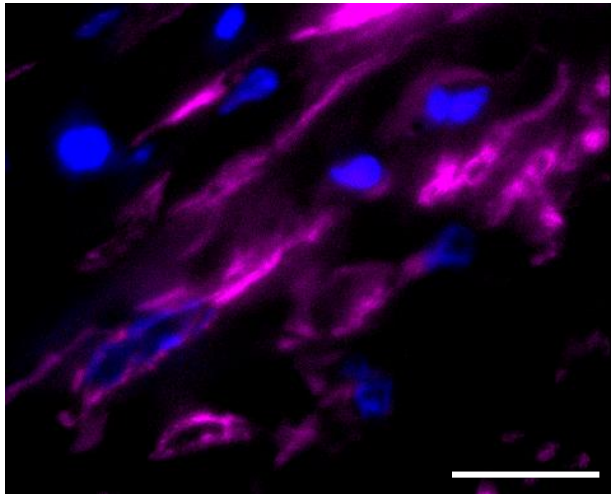

I

TNC / αSMA / DAPI

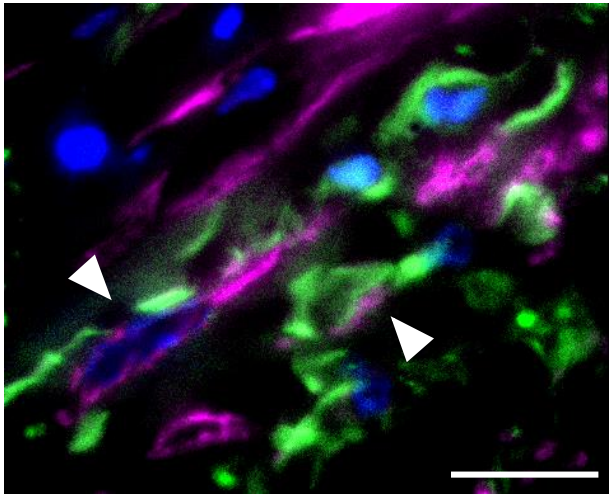

J

Figure2

Fig. 2

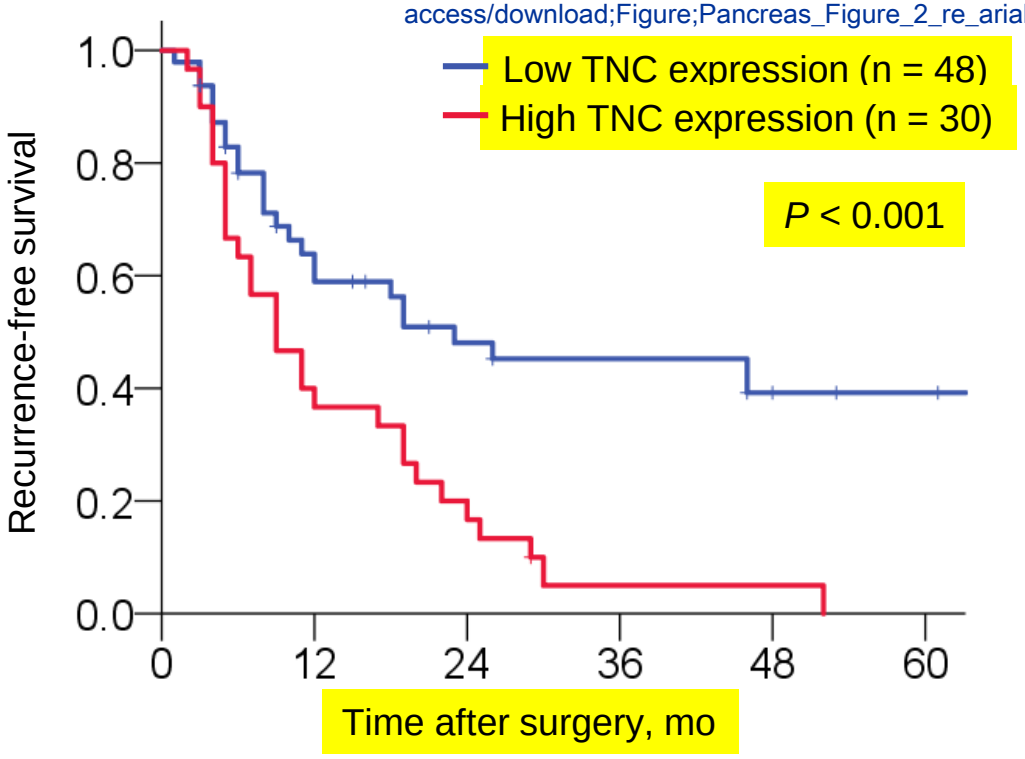

Number at risk

Low	48	24	15	10
High	30	11	1	0

A

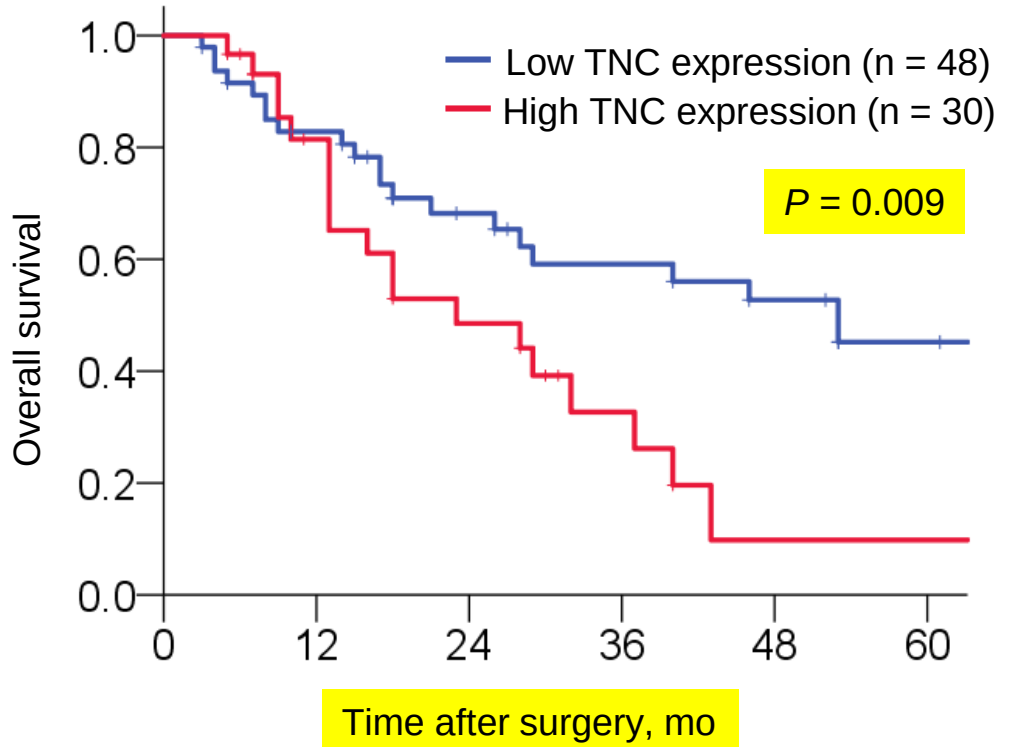

Number at risk

Low	48	37	19	10
High	30	20	5	1

B

Fig. 3

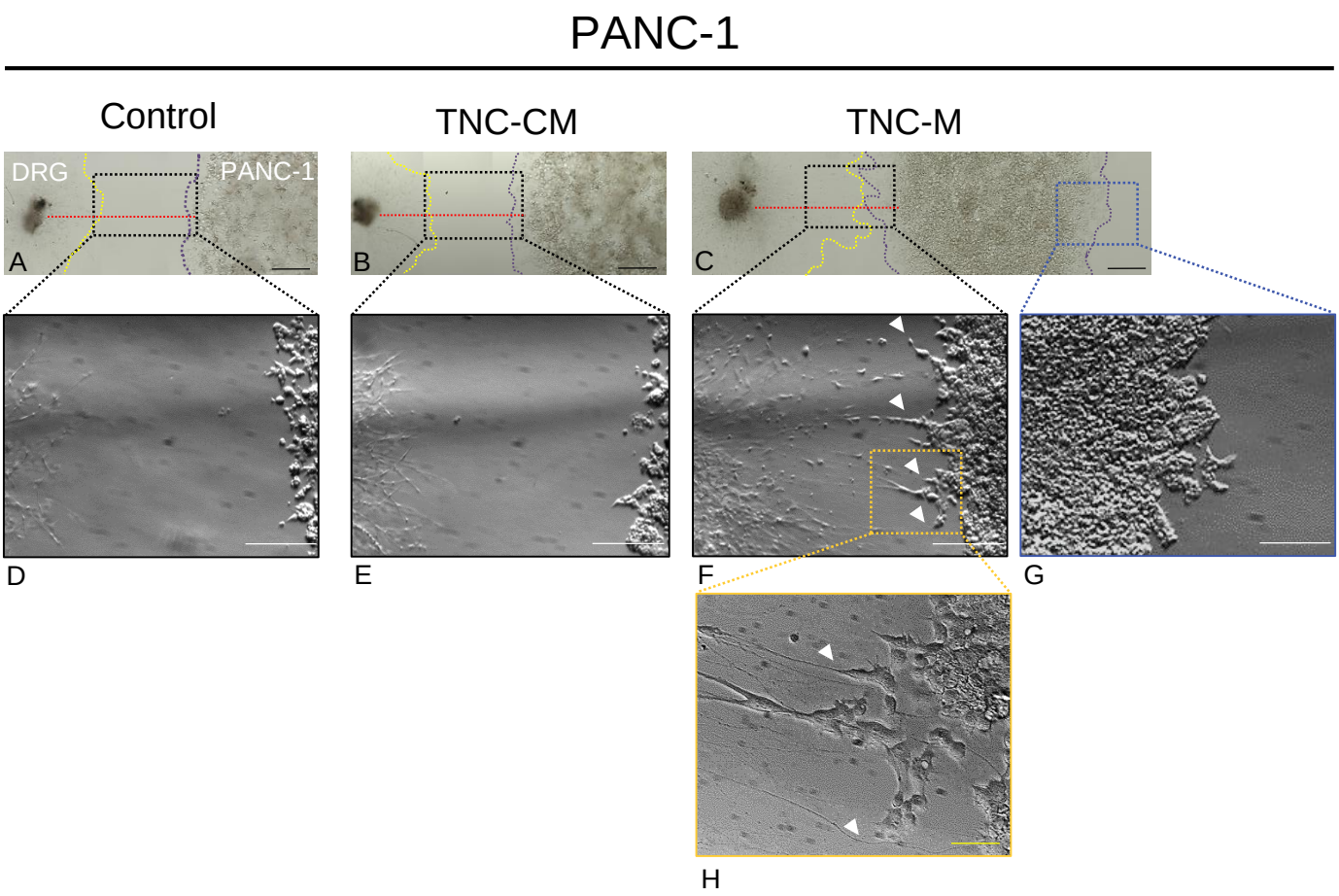

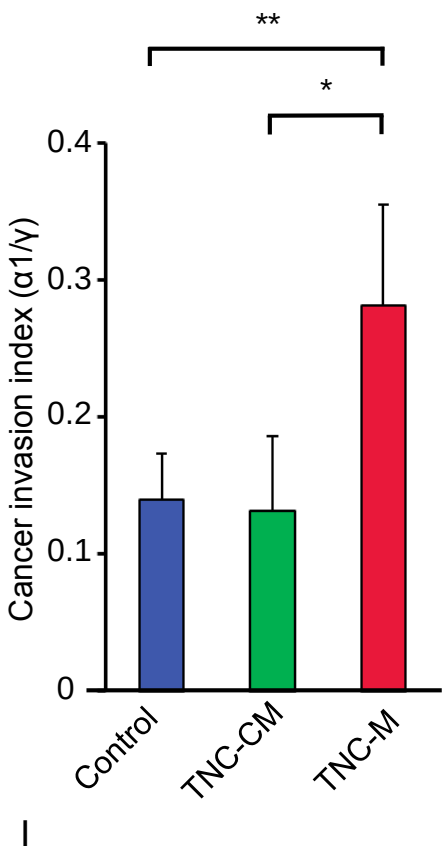

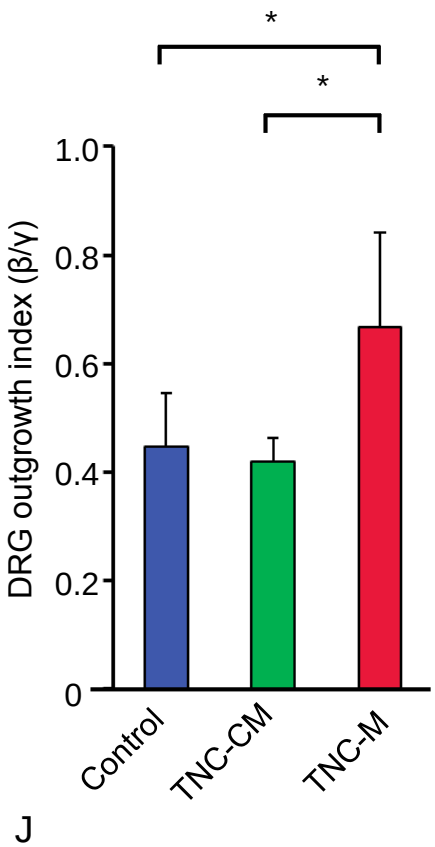

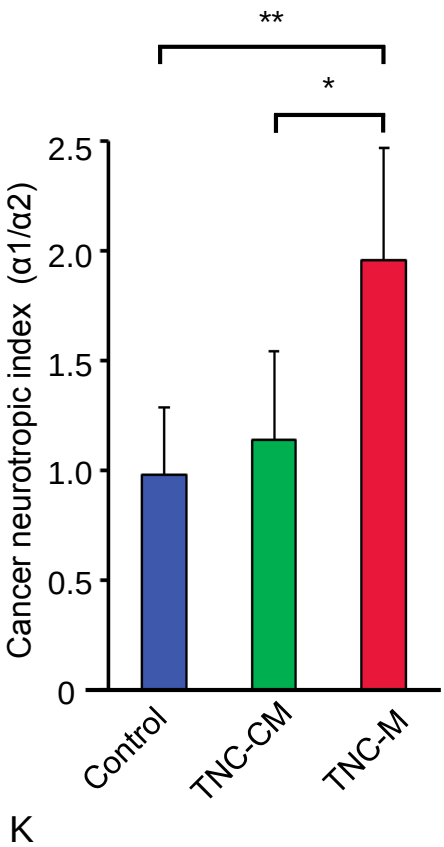

Fig. 3

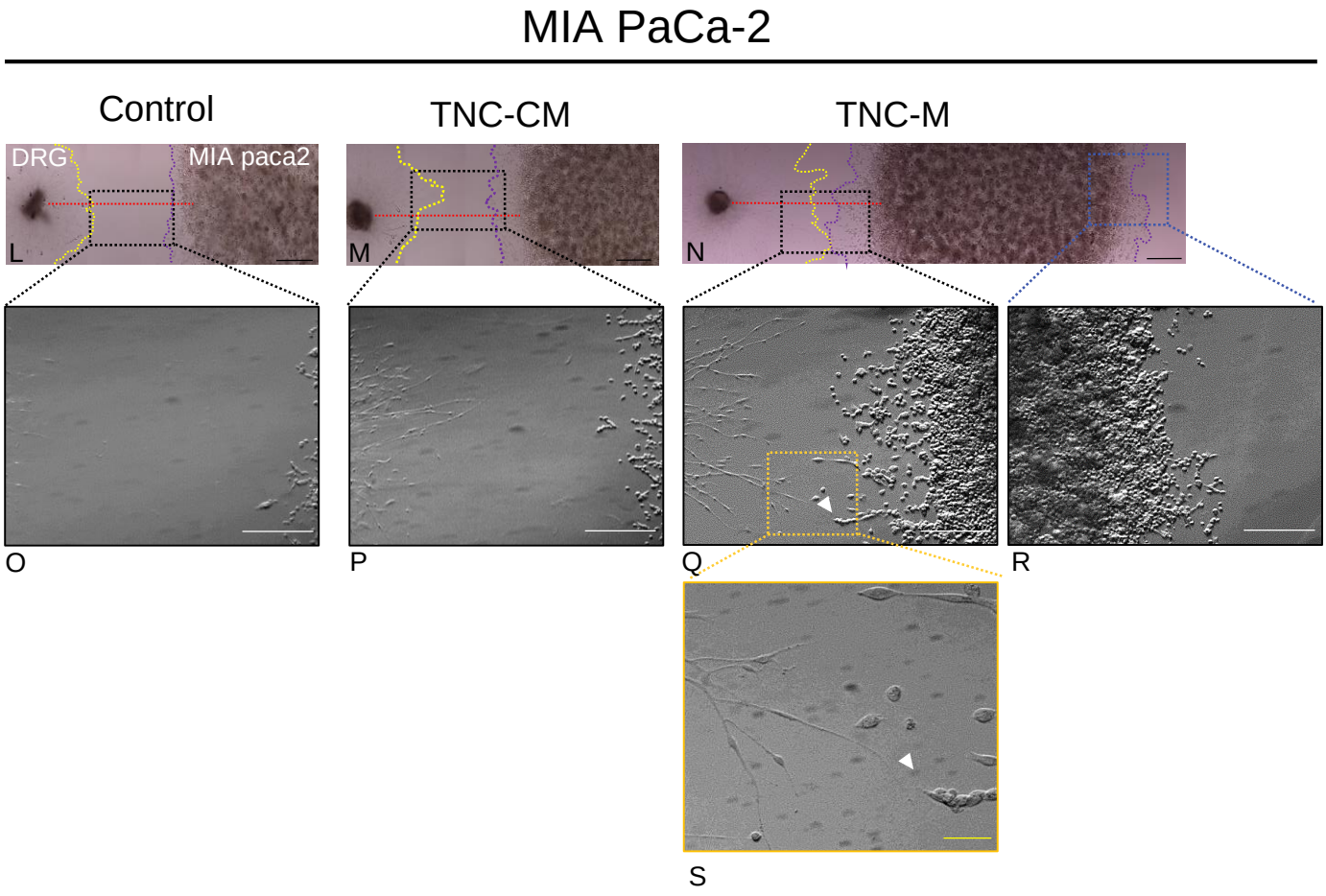
MIA PaCa-2
Control
TNC-CM
TNC-M
DRG
MIA paca2
L
M
N
O
P
Q
R
S

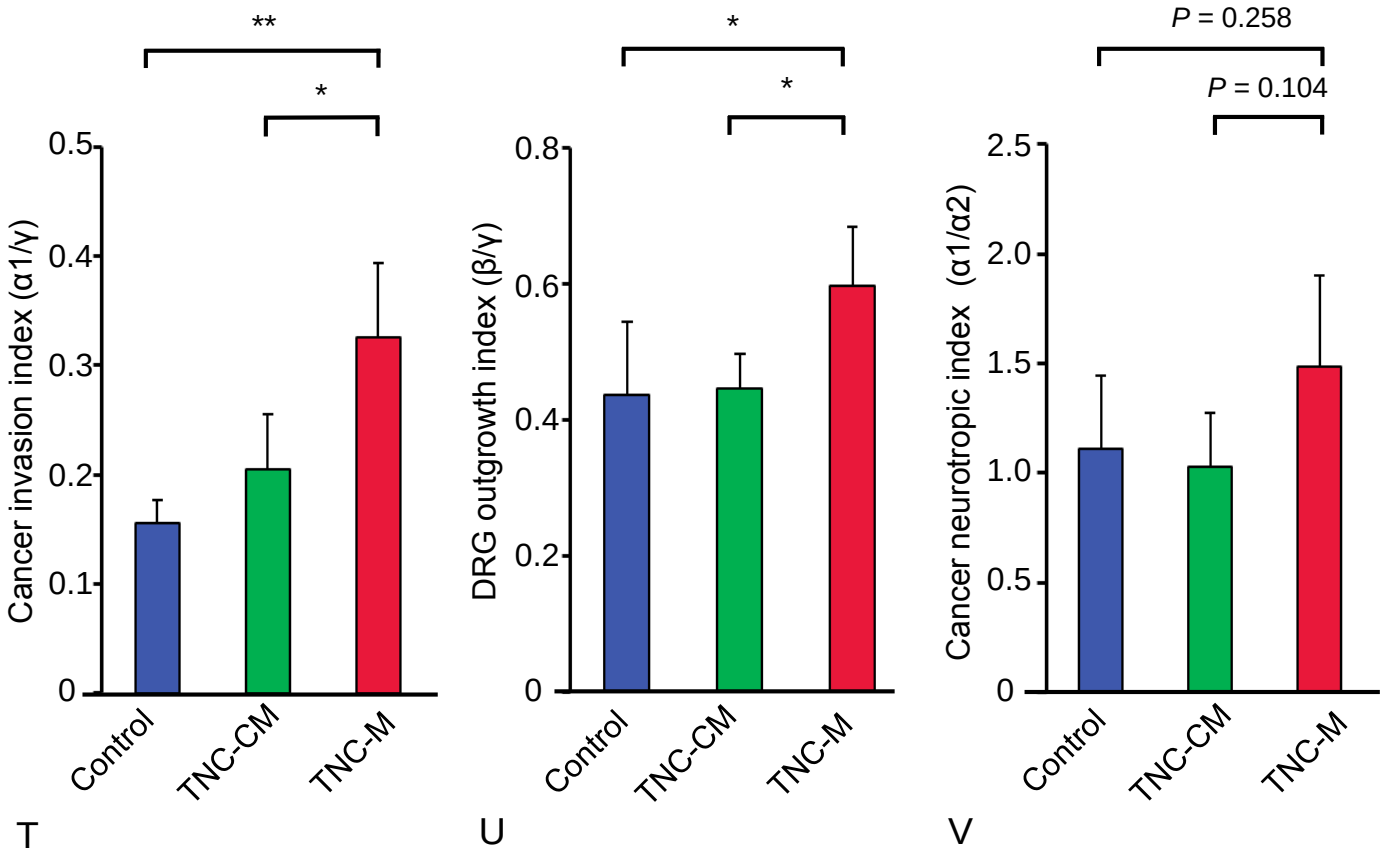
**
*
Cancer invasion index (α1/γ)
0
0.1
0.2
0.3
0.4
0.5
Control
TNC-CM
TNC-M
T
*
*
DRG outgrowth index (β/γ)
0
0.2
0.4
0.6
0.8
Control
TNC-CM
TNC-M
U
P = 0.258
P = 0.104
Cancer neurotropic index (α1/α2)
0
0.5
1.0
1.5
2.0
2.5
Control
TNC-CM
TNC-M
V

Fig. 4

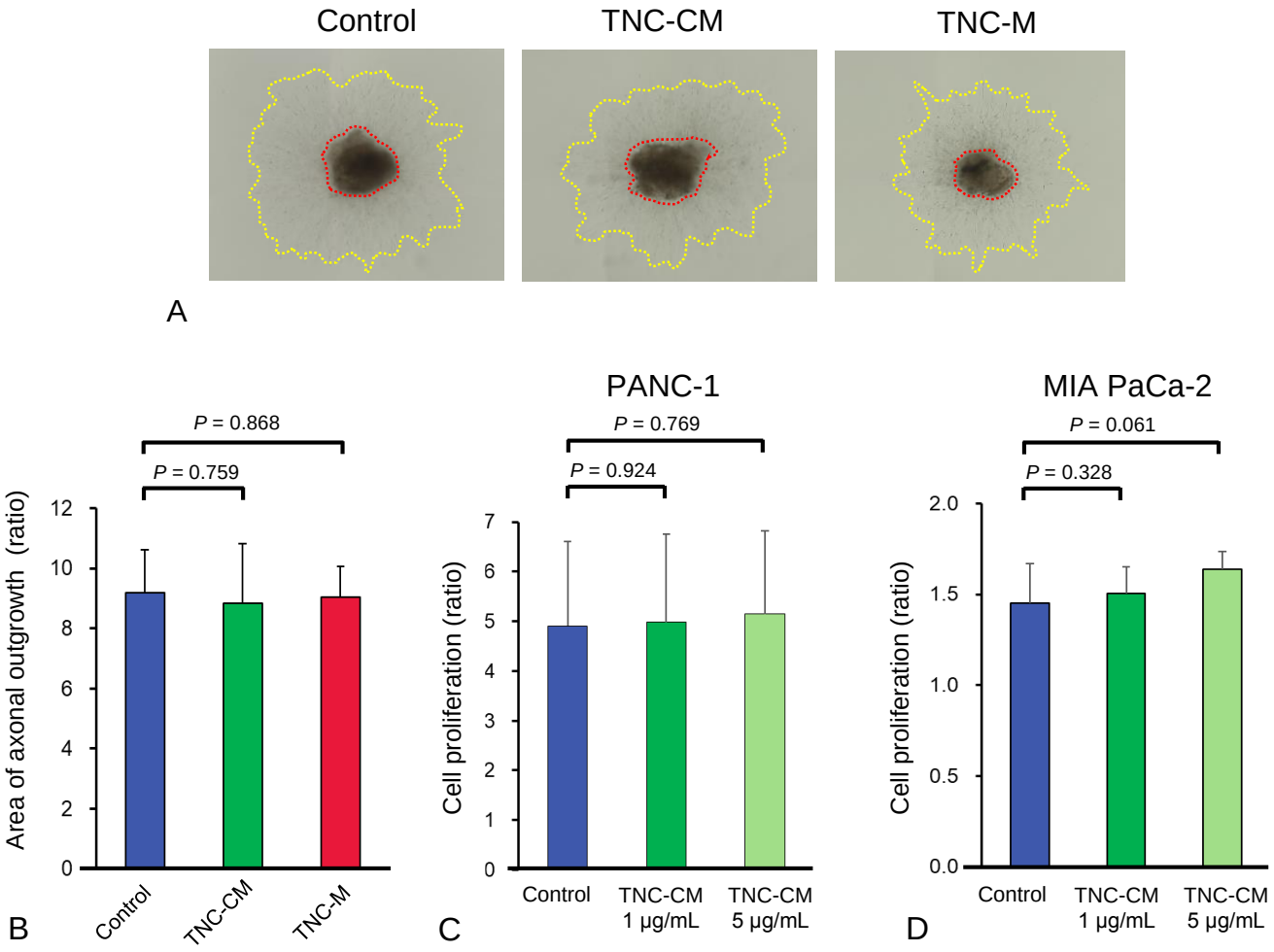

Fig. 5

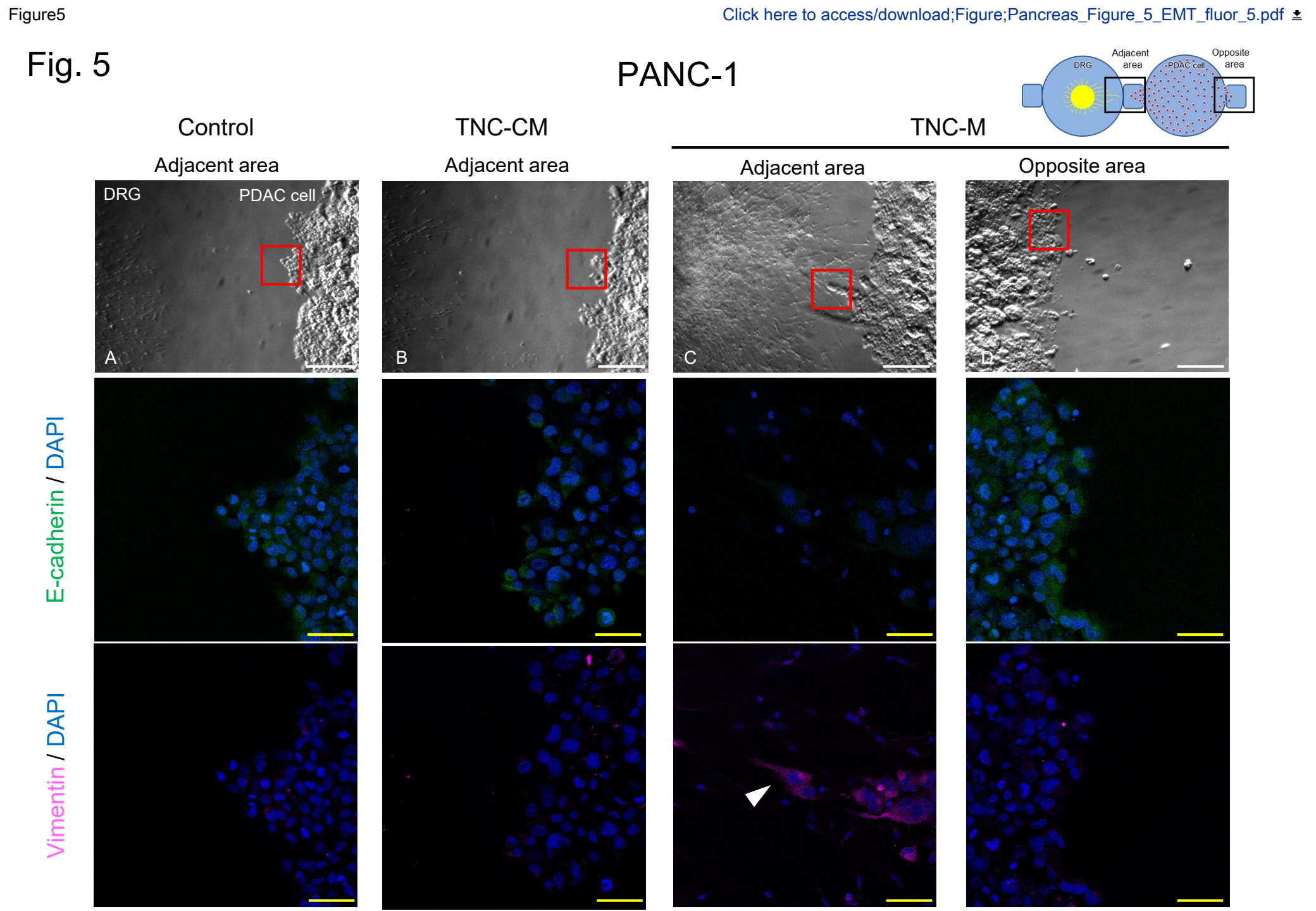

Fig. 5

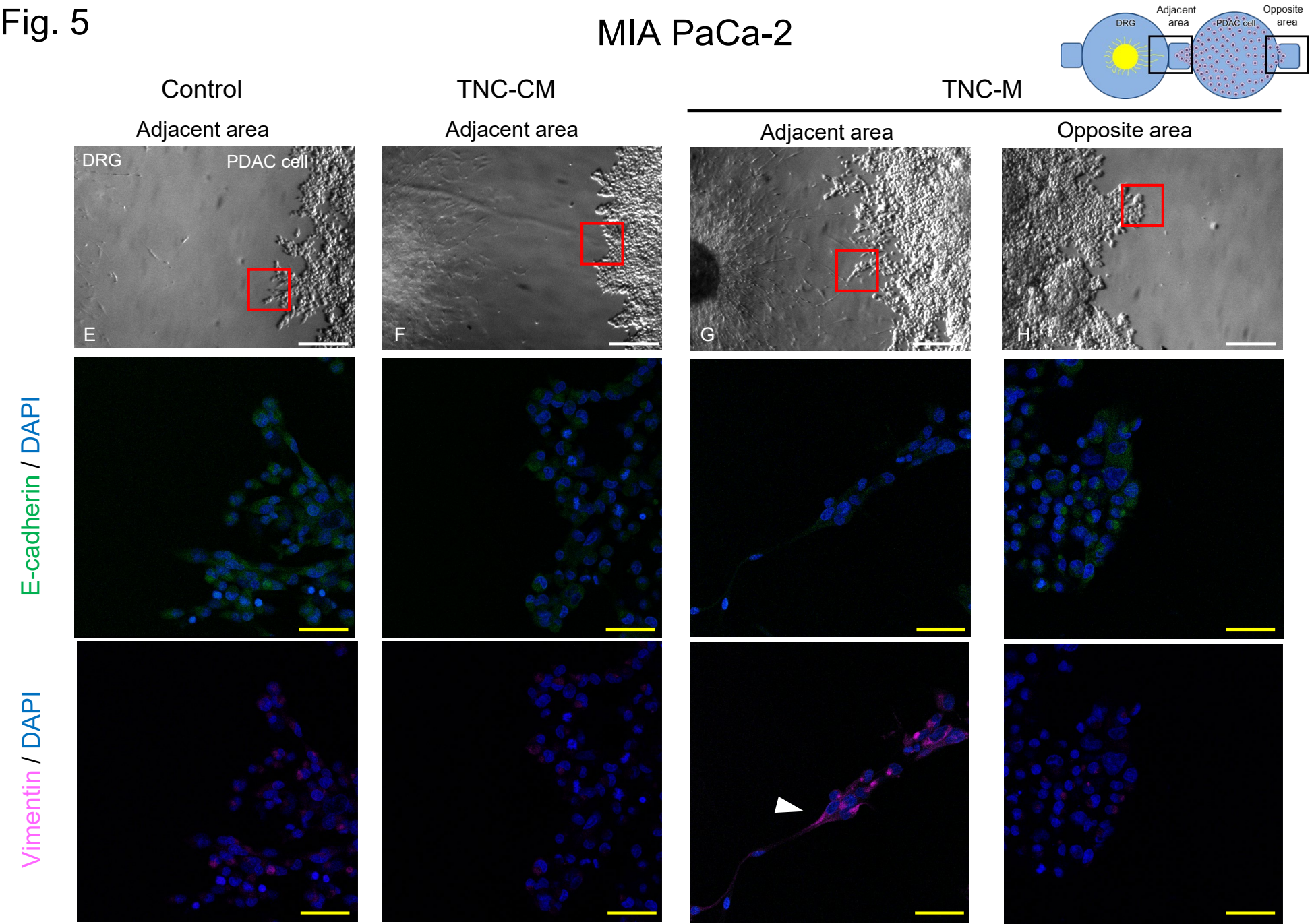
MIA PaCa-2
DRG
Adjacent area
PDAC cell
Opposite area
Control
TNC-CM
TNC-M
Adjacent area
Adjacent area
Opposite area
DRG
PDAC cell
E
F
G
H
E-cadherin / DAPI
Vimentin / DAPI

Figure6

Fig. 6

Click here to access/download;Figure;Pancreas_Figure_6_PSC_pdf.pdf

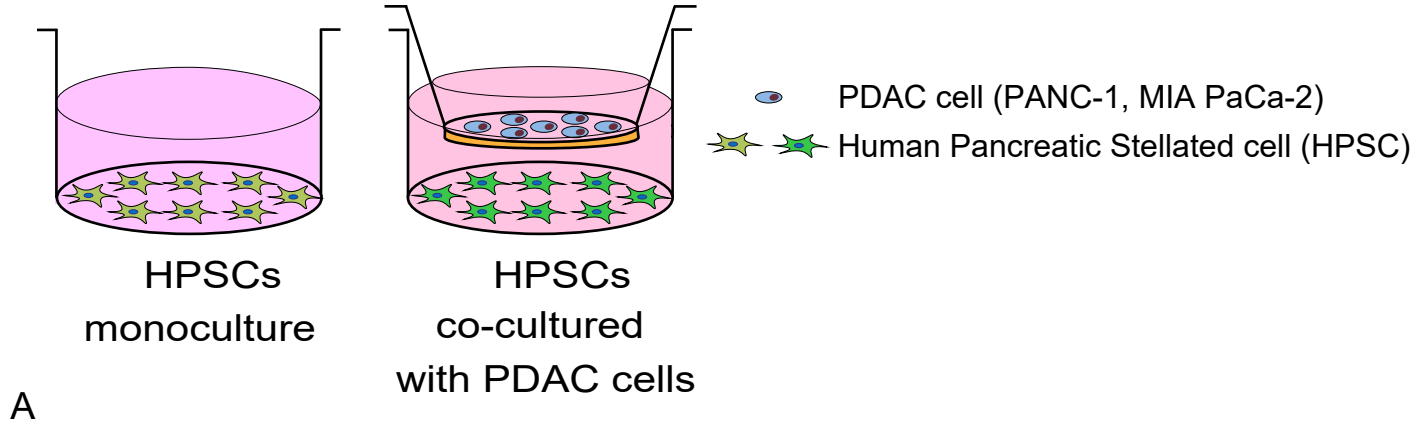

A

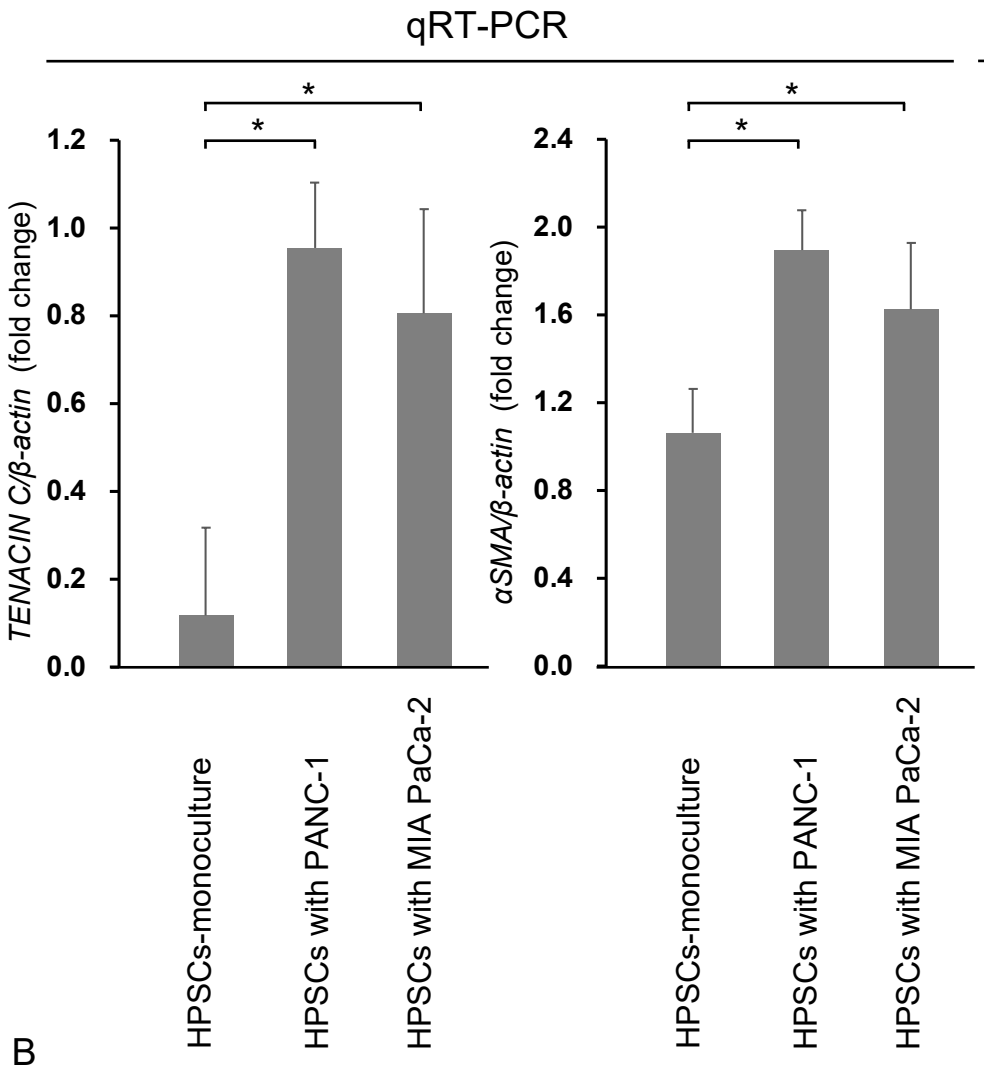

B

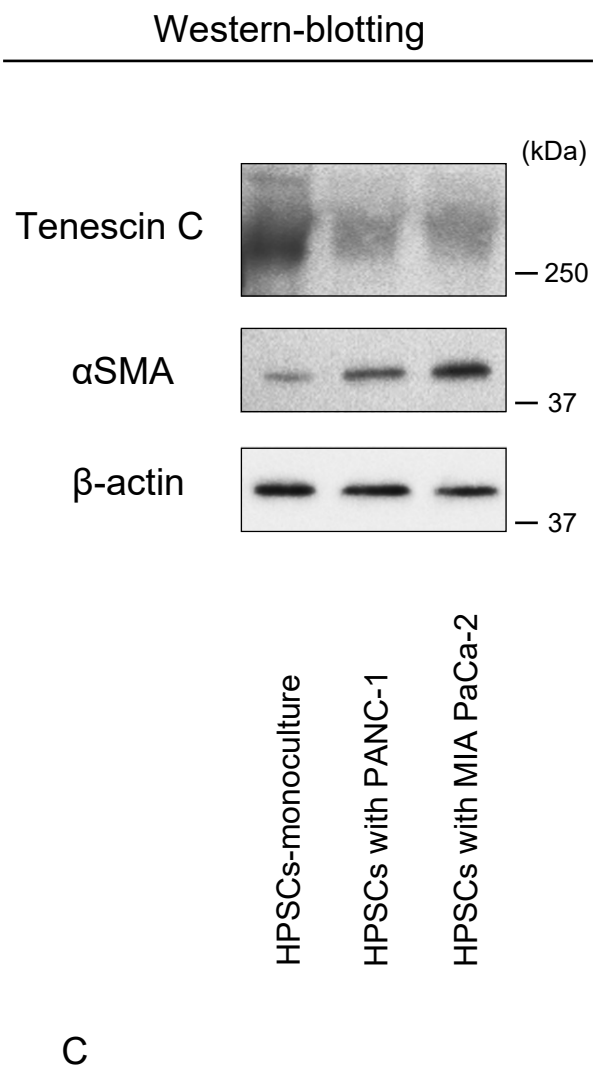

C

Table1

Table 1. Relationships Between Clinicopathological Features and Tenascin C (TNC) Expression in Perineural Sites

		Tenascin C expression		P
	Total (n = 78)	**Low (n = 48)**	**High (n = 30)**	
Age, mean (SD), y	68.2 (8.6)	67.6 (8.8)	69.5 (8.3)	0.247
Sex				
Male	37	25	12	0.298
Female	41	23	18	
CA 19-9, median, U/mL				
<77	39	25	14	0.774
≥77	40	24	16	
Tumor location				
Head	56	31	25	0.073
Body/tail	22	17	5	
Tumor size, cm				
<2	20	15	5	0.151
≥2	58	33	25	
UICC grade				
G1/G2	74	45	29	0.656
G3	4	3	1	
Lymphatic invasion				
Absent	49	33	16	0.17
Present	29	15	14	
Vascular invasion				
Absent	22	16	6	0.203
Present	56	32	24	
Perineural invasion				
Absent	24	20	4	0.008
Present	54	28	26	
UICC pT				
1,2	8	8	0	0.021
3,4	70	40	30	
UICC pN				

0	23	15	8	0.666
1,2	55	33	22	
UICC pStage				
≤IIA	22	15	7	0.45
≥IIB	56	33	23	
Curability				
R0	63	41	22	0.188
R1	15	7	8	
Postoperative chemotherapy				
Yes	52	33	19	0.622
No	26	15	11	
αSMA expression in perineural sites				
Low	47	40	7	< 0.001
High	31	8	23	

SD standard deviation, *CA19-9 carbohydrate antigen 19-9*, *UICC* the Union for International Cancer Control, *G* histological grade, *p* pathological, *T* primary tumor, *N* nodal status, *R0* no residual tumor, *R1* microscopic residual tumor, *αSMA* alpha smooth muscle actin

Table2

Table 2: Uni- and Multi-Variate Analyses of Prognostic Factors Associated With Recurrence-Free Survival

			Univariate		Multivariate	
Variables	**n**	**5-yr, %**	**Hazard ratio (95% CI)**	**P**	**Hazard ratio (95% CI)**	**P**
Age, y						
<69	38	26.7				
≥69	40	17.1	1.044 (0.608–1.795)	0.875		
Sex						
Male	37	24.6				
Female	41	21.6	1.193 (0.696–2.045)	0.522		
CA 19-9, U/mL						
<77	38	35.4				
≥77	40	11.2	1.983 (1.146–3.432)	0.014	1.205 (0.649–2.235)	0.555
Location						
Body/tail	22	41.3				
Head	56	16.9	1.921 (0.987–3.737)	0.055		
UICC grade						
G1/G2	74	23.8				
G3	4	0	2.258 (1.324–3.852)	0.003	2.230 (1.203–4.136)	0.011
Lymphatic invasion						
Absent	49	30.3				
Present	29	9.6	2.335 (1.359–4.013)	0.002	1.612 (0.857–3.031)	0.138
Perineural invasion						
Absent	24	53.5				
Present	54	8.3	3.689 (1.837–7.408)	< 0.001	3.532(1.637–7.618)	0.001
UICC pT						
1,2	8	66.7				
3,4	70	17.8	5.172 (1.254–21.322)	0.023	2.292 (0.506–10.380)	0.282
UICC pN						
0	23	41.2				
1,2	55	14.3	2.825 (1.447–5.515)	0.002	1.001(0.126–7.930)	0.999

UICC pStage						
≤IIA	22	43.1				
≥IIB	56	14.0	3.080 (1.538–6.168)	0.001	2.742 (0.322–23.338)	0.356
Curability						
R0	63	27.2				
R1	15	6.7	2.023 (1.098–3.729)	0.024	0.776 (0.361–1.665)	0.514
Tenascin C expression						
Low	48	39.2				
High	30	0	2.432 (1.462–4.387)	0.001	2.202 (1.019–4.758)	0.045
αSMA expression						
Low	47	35.9				
High	31	4.8	1.889 (1.098–3.250)	0.022	0.829 (0.357–1.926)	0.663

CI confidence interval, *CA19-9* carbohydrate antigen 19-9, *G* histological grade, *UICC* the Union for International Cancer Control, *p* pathological, *T* primary tumor, *N* nodal status, *R0* no residual tumor, *R1* microscopic residual tumor, *αSMA* alpha smooth muscle actin

Table 3 Correlations Between Tenascin C (TNC) Expression in Perineural Sites qWith Recurrence Pattern

Recurrence pattern	Tenascin C expression		P
	Low (n = 29)	High (n = 37)	
Locoregional	10	29	0.002
Distant (LN, liver, lung, bone)	12	4	
Peritoneal	7	4	

Numbers include overlapping cases.

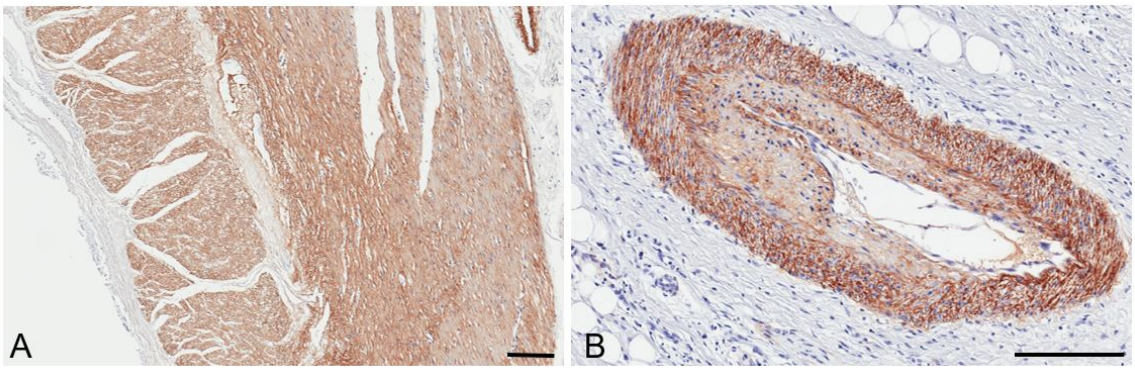

Figure S1. Immunohistochemical staining of Tenascin C for smooth muscle (**A**) and vessel wall (**B**) in PDAC specimens as postivie control are shown. Scale bar: 200 µm.

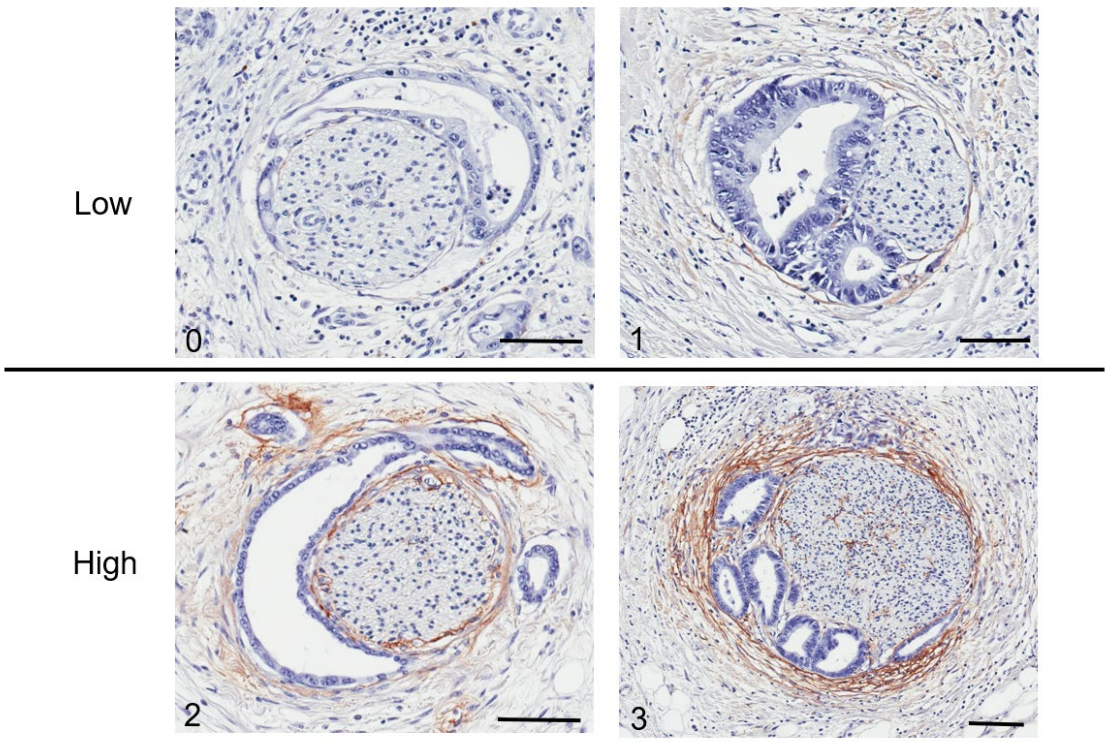

Figure S2. Representative immunostaining of tenascin C (TNC) in perineural sites. TNC staining intensity was classified according to four scores: 0, negative or obscure; 1, weak; 2, moderate and 3, strong. Additionally, TNC expression was classified as being either low (0,1) or high (2, 3). Scale bar: 100 μm

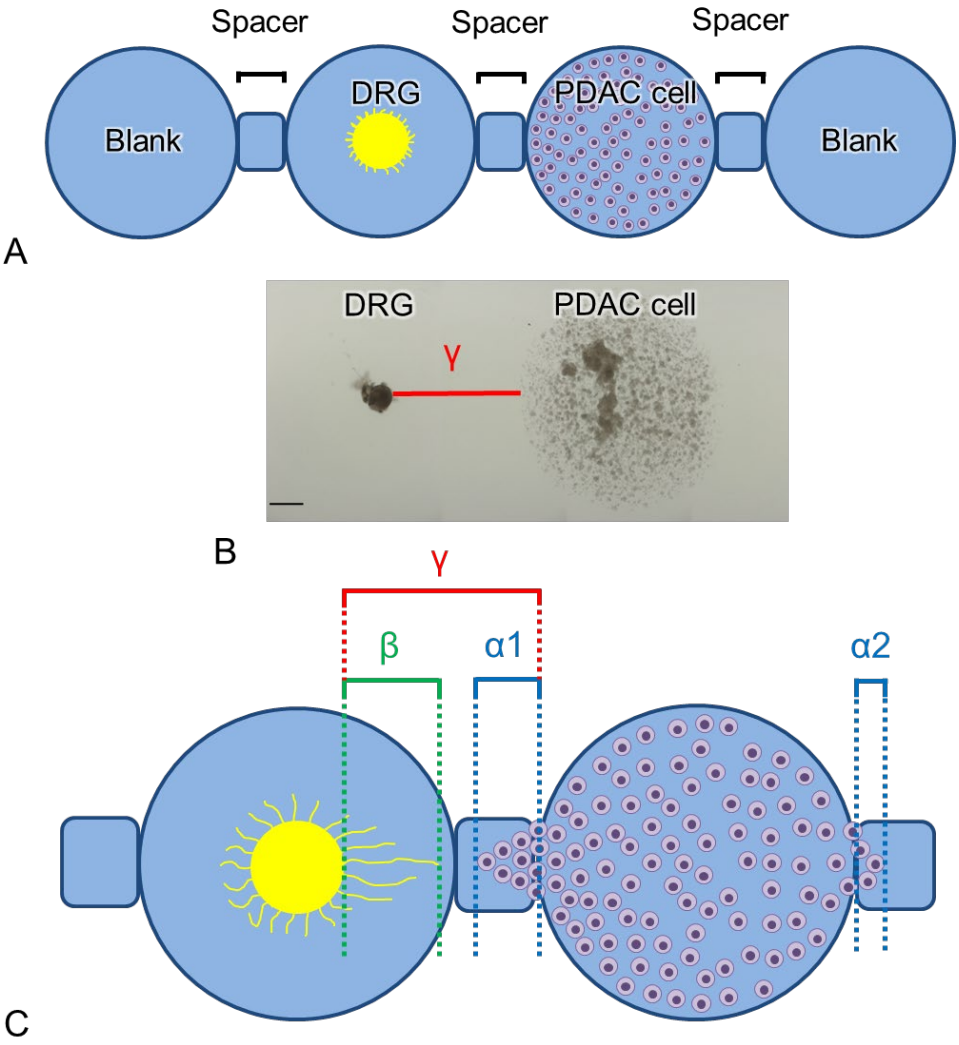

Figure S3. Illustrations of *in vitro* co-culture model. (**A**) Schematic representation of *in vitro* co-culture model with pancreatic ductal adenocarcinoma (PDAC) cells and a dorsal root ganglion (DRG). PANC-1 or MIA paca2 cells (50,000 cells suspended in 5 μL solidified Matrigel) were placed next to DRG suspension. An additional 5 μL "blank" Matrigel was positioned on the opposite sides. Each cell-suspended or blank Matrigel was connected by a 1-mm-long Matrigel plug ("Spacer"). (**B**) A photographic image of *in vitro* co-culture model on day 0; γ: minimum distance between edges of PDAC cell-suspended Matrigel and DRG (scale bar: 100 μm). (**C**) Illustration showing calculation of cancer invasion index (α1/γ), DRG outgrowth index (β/γ), and cancer neurotropic index (α1/α2).

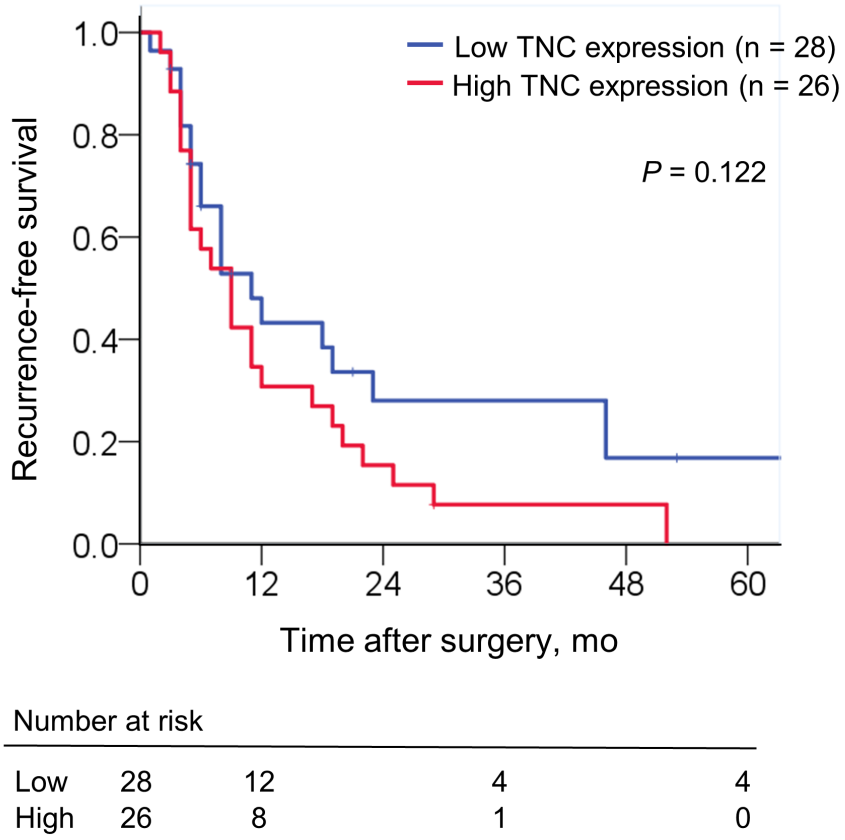

Figure S4. Kaplan-Meier survival curves of recurrence-free survival for patients with presense of perineural invasion (n = 54), stratified by tenascin C (TNC)-expression pattern in perineural sites.